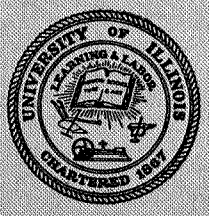

UNIVERSITY OF ILLINOIS
URBANA

AERONOMY REPORT NO. 7

AN AUTOMATIC RECORDING SYSTEM FOR THE DETERMINATION OF IONOSPHERIC ABSORPTION

by
Robert L. Appel
S. A. Bowhill

September 1, 1965

Supported by
National Aeronautics and
Space Administration
Grant NSG-511

Aeronomy Laboratory
Department of Electrical Engineering
University of Illinois
Urbana, Illinois

CITATION POLICY

Since much of the material in this report may be published in accepted aeronomic journals, it would be appreciated if persons wishing to cite work contained herein would first contact the authors to ascertain if the relevant material is part of a paper published or in process.

AERONOMY REPORT NO. 7

AN AUTOMATIC RECORDING SYSTEM FOB THE DETERMINATION OF IONOSPHERIC ABSORPTION

by

Robert L. Appel

S. A, Bowhill

September 1, 1965

Supported by
National Aeronautics and
Space Administration
Grant NSG–511

Aeronomy Laboratory
Department of Electrical Engineering
University of Illinois
Urbana, Illinois

ACKNOWLEDGEMENT.

The author wishes to express sincere appreciation to his advisor, Professor S. A. Bowhill, for his helpful advice and guidance throughout the course of the research work. The author is grateful to Mr. G. W. Henry for his assistance with the project and to Mr. J. Russell for constructing the experimental system. Thanks are also due to Mrs. J. Potter for typing the final report.

The research described in this document has been sponsored by the National Aeronautics and Space Administration under grant NsG-511.

ABSTRACT

The design and operation of an automatic recording system for the analysis of ionospheric absorption measurements is discussed. The system is intended to replace the visual measurement equipment presently being used by the Aeronomy Laboratory at the University of Illinois.

The automatic recording system gives absorption measurements which are proportional to the mean amplitude of the reflected signal. In addition, the apparent reflection height of the transmitted wave is automatically determined. Two methods of recording the obtained data are described, as well as various applications of the proposed system,

TABLE OF CONTENTS

TABLE OF CONTENTS (continued)

LIST OF ILLUSTRATIONS

1. INTRODUCTION

1.1 The Ionosphere

The term ionosphere was first applied by Sir Robert Watson-Watt to that part of the earth's atmosphere in which free electrons exist in sufficient quantities to affect the propagation of radio waves,, The ionosphere may therefore be considered as the region lying between about 50 and 1000 km above the surface of the earth. The dominant feature of this region is its relatively high value of electrical conductivity resulting from the presence of the free electrons and the low gas pressures present in this height range.

It was once thought that the electron density varied irregularly with height and that distinct layers of electrons would tend to form in different regions. Based on this hypothesis, the ionosphere was divided into three maximum density regions as follows: D-region, from 50 to 90 km; E-region, from 90 to 160 km; and F-region, above 160 km.

However, rocket measurements have since established that the variation of electron density with height is not necessarily characterized by well-defined peaks, but is sometimes distinguished only by a very small gradient of electron density with height, The electron density is, therefore, considered to increase continuously with height throughout the entire ionosphere. It is still convenient, however, to retain the region designations previously mentioned and to refer, for example, to any electron density peak occurring within the E-region as the E-layer,

Since the ionosphere is a highly conductive region, there is essentially no net charge density and the electrons must be accompanied by an equal number

of positively charged gaseous ions, which may be either atomic or molecular. The ions and electrons are primarily produced by ultraviolet radiation from the sun which ionizes the existing gas molecules and atoms in a particular region,

As the ionizing radiation penetrates deeper and deeper into the ionosphere, it encounters a gradually increasing gas density, thus producing an increasing number of electrons in each unit volume. The radiation, however, is continually being absorbed in the process. Eventually a point is reached where the decrease in the radiation intensity is greater than the increase in the gas density, so that the rate of electron production begins to decrease as the radiation penetrates still farther into the atmosphere. Thus, there exists a level at which the production of electrons is a maximum, and it is determined jointly by the degree of absorption of the radiation and by the variation in the gas density,

The problem of determining the rate of production at each level is a good deal more complicated, since the atmosphere is composed of many different gases and the solar spectrum covers a wide range of wavelengths. The simplest type of ionized layer that can be deduced from theoretical considerations was proposed by Chapman (1931). His derivation was based on the following assumptions:

(i) An atmosphere with only one type of gas,
(ii) Plane stratification (flat earth).
(iii) A parallel beam of monochromatic ionizing radiation from the sun,
(iv) An isothermal atmosphere,

The theory clearly demonstrates the existence of a maximum density layer as predicted.

1.2 Ionospheric Radio Wave Propagation

Having briefly discussed the general properties of the ionosphere, it is now possible to consider the propagation of an electromagnetic wave through this

particular type of medium. For simplicity, it will be assumed that the region has a constant ionization density and is not influenced by the earth's magnetic field. The electric field E is defined by

$$E = E_o \sin 2\pi ft \tag{1.1}$$

where E_o is the magnitude of the field and f is the propagation frequency. The force exerted on each free electron of charge -e is -eE. If v is the electron velocity, Newton's second law for the motion of an electron with mass m may be written as

$$m \frac{dv}{dt} = -eE_o \sin 2\pi ft. \tag{1.2}$$

Integration of equation (1.2) gives an expression for the eleetron velocity as

$$v = \frac{eE_o}{2\pi mf} \cos 2\pi ft. \tag{1.3}$$

Assuming that the electron density is N electrons per unit volume, the electron movement will produce a convection current density J_c given by

$$J_e = Nev. \tag{1.4}$$

Substitution of equation (1.3) into this expression yields

$$J_c = \frac{-NE_o e^2}{2\pi mf} \cos 2\pi ft. \tag{1.5}$$

In addition to the convection current produced, the ohanging electric field will also give a displacement current density J_d given by

$$J_d = \varepsilon_o \frac{dE}{dt} = \varepsilon_o E_o \frac{d}{dt} \sin 2\pi ft \tag{1.6}$$

or,

$$J_d = 2\pi f \varepsilon_o E_o \cos 2\pi ft \tag{1.7}$$

where ε_o is the dielectric constant of the medium in the absence of electrons.

The total current density J produced as a result of the wave propagating through the medium is simply the sum of the convection current density J_c and the displacement current density J_d. Prom equations (1.5) and (1.7), the total current density may be expressed as

$$J = 2\pi f \varepsilon_o E_o \cos 2\pi ft - \frac{NE_o e^a}{2\pi mf} \cos 2\pi ft \tag{1.8}$$

which can be written in the form

$$J = \varepsilon \quad \frac{Ne}{4\pi^2 \varepsilon mf^2} \; 2\pi fE \cos 2\pi ft. \tag{1.9}$$

It is readily apparent from a comparison of equations (1.7) and (1.9) that as a result of the presence of free electrons, the dielectric constant E of the ionosphere has been reduced from ε_o to $\varepsilon_o (1 - Ne^a/4\pi^2 \varepsilon_o mf^2)$.

In a non-absorbing medium, moreover, the phase refractive index μ is equal to the square root of the ratio of the dielectric constant of the medium E and the dielectric constant of free space E_o. Hence, the phase refractive index μ of the ionosphere may be given as

$$\mu = \left(1 - \frac{Ne^2}{4\pi^2 \varepsilon_o mf^2}\right)^{\frac{1}{2}}. \tag{1.10}$$

Substituting for the constant terms in equation $1.10), the phase refractive index of the ionosphere can be written as

$$\mu = (1 - 80.62\ N/f^2)^{\frac{1}{2}} \qquad (1.11)$$

where both N and f are expressed in MKS units'.

From this expression, it is readily apparent that if a radio wave passes into a region such as the ionosphere, in which the electron density N is steadily increasing with height, the refractive index will decrease according to equation (1.11). Moreover, at a sufficiently low frequency it may attain the condition $\mu = 0$. At this condition, the transmitted wave frequency is equal to the plasma frequency, f_N, and at that particular level

$$f_N = 8.979\ N^{\frac{1}{2}}. \qquad (1.12)$$

No wave of frequency less than f_N can propagate in a simple plasma and the wave is thenefore reflected. At vertical incidence, waves below approximately 10 Mc/s will be reflected (excluding the critical penetration frequencies), while all others will propagate through the ionosphere and escape into outer space.

At oblique incidence, it is necessary to divide the ionosphere into a number of horizontal slabs of uniform density. If Snell's Law is applied at each interface, the wave will be reflected when the wave refractive index μ is equal to $\sin i$, i being the angle of incidence of the wave with the ionized layer. This process is analogous to total internal reflection in optics. The multiple reflection of electromagnetic waves is essentially the property on which all forms of long-distance radio communications are based. Waves above approximately 20 Mc/s will propagate through the ionosphere at oblique incidence, while all frequencies below will be reflected.

1.3 Theory of Ionospheric Absorption

The complete magneto-ionic theory of ionospheric absorption is a subject of some complexity, and only a brief discussion will be included here. A rather thorough treatment of the theory is given by Davies (1965), in which he considers both the effect of a magnetic field and the presence of electron collisions.

In its simplest sense, the absorption of an electromagnetic wave propagating through the ionosphere can be considered as the extraction of a portion of the wave's energy by electron collisions, The field of the wave causes the electrons to oscillate at the same frequency as the field and to dissipate energy as the vibrating electrons collide with other particles or with each other. This energy is given off in the form of heat and random radiation.

The rate of loss of the wave energy is dependent upon the average kinetic energy of vibration of the electrons and the number of electron collisions which occur per unit volume in unit time. The latter is clearly equal to the product of the existing electron density, N, and the electron collisional frequency ν. It is important to note at this time that absorption measurements generally can give information only about this product $N \cdot \nu$. If an electron density profile is the desired result, some assumption must be made regarding the collisional. frequency ν based on its measurement by another method.

Since the end result of absorption is the attenuation of the propagated wave, it has become common practice to speak of an absorption coefficient κ per unit thickness of the absorbing medium. If an electromagnetic wave has an amplitude I after transversing a distance s in the medium, the amplitude of the received signal can be given as

$$I = I'_0 \exp(-\kappa s) \qquad (1.13)$$

where I'_o is the amplitude of the wave which would have been observed if the medium did not absorb. Since the absorption coefficient κ in the ionosphere varies along the wave-path, it is possible to measure the total absorption, $\int \kappa ds$, only between two points in the path where

$$\int \kappa ds = -\ln (I/I'_o) \qquad (1.14)$$

The magneto-ionic theory also shows that, provided the direction of phase propagation is not perpendicular to the earth's magnetic field, the absorption coefficient κ of high frequency waves depends on the refractive index μ, the electron density N, the electron collisional frequency ν, the dielectric constant of free space ε_o, and on the electronic charge and mass, e and m, according to the equation

$$\kappa = \frac{e^2}{2\varepsilon_o mc} \cdot \frac{1}{\mu} \cdot \frac{N\nu}{\nu^2 + (\omega \pm \omega_L)^2} \qquad (1.15)$$

where c is the velocity of electromagnetic waves in a vacuum (i.e. the speed of light), ω is the angular frequency of the transmitted wave, ω_L is the angular gyro-frequency of the longitudinal component of the earth's magnetic field, and the positive and negative signs refer to the ordinary and extraordinary modes of propagation respectively.

It should be mentioned that at or near a reflection point, the direction of propagation of the ordinary wave becomes transverse to the earth's magnetic field, and, at this condition, equation (1.15) is not strictly applicable. It is also apparent from an inspection of equation (1.15) that the extraordinary wave is more greatly absorbed or attenuated than the ordinary wave, the degree of difference of attenuation in the two modes of Propagation depending on the

relative values of the transmitting angular frequency ω, and the angular gyro-frequency ω_L.

1.4 Deviative Absorption

A radio wave propagating through the ionosphere will experience a continually decreasing phase refractive index μ with increasing height. Considering the ionosphere as being divided into a number of horizontal slabs of uniform density, Snell's law may be applied at each interface and can be expressed by

$$\sin i = \mu \sin i' \tag{1.16}$$

where i is the angle of incidence of the propagated wave with the ionosphere and i' is the angle of the wave at each interface. From this expression, it is apparent that as the angle i' increases with height, the phase refractive index μ will decrease. Moreover, at the condition $i' = 90^{\circ}$, the phase refractive index μ will be equal to sin i and the wave is reflected at this height. The absorption which occurs in regions where μ is small and where a deviation or bending of the signal path exists has been termed deviative absorption.

If it is assumed that the angular transmission frequency ω is large compared to the angular gyro-frequency ω_L, equation (1.15) for small values of μ may be written as

$$\kappa = \frac{e^2}{2\varepsilon_o mc} \cdot \frac{1}{\mu} \cdot \frac{N\nu}{\nu^2 + \omega^2} . \tag{1.17}$$

Furthermore, the operating frequency ω is usually much larger than the collisional frequency ν. Hence, equation (1.17) may be written as

$$\kappa = \frac{e^2}{2\varepsilon_o mc} \cdot \frac{1}{\mu} \cdot \frac{N\nu}{\omega^2} . \tag{1.18}$$

The phase refractive index μ was given by equation (1.10). Squaring this equation and substituting $2\pi f$ for ω yields

$$\mu^2 = 1 - \frac{Ne^2}{\varepsilon m\omega^2} \tag{1.19}$$

Combining equations (1.18) and (1.19) gives

$$\kappa = \frac{\nu}{2c}\left(\frac{1}{\mu} - \mu\right). \tag{1.20}$$

It is readily apparent from this expression that the absorption coefficient κ and hence the total absorption, $\int \kappa ds$, will depend critically on the value of the refractive index μ, when μ is small.

1.5 Non-Deviative Absorption

An inspection of equation (1.16) also reveals that when the phase refractive index μ is equal to unity, the transmitted wave will propagate through the medium at essentially the speed of light. Hence, in regions where μ is approximately unity, there will be little or no deviation of the transmitted signal from its free-space path. This type of absorption is called non-deviative absorption and occurs primarily in the D-region of the ionosphere, whereas for proper selection of the transmitting frequency, deviative absorption will occur in the E-region, where a reflection of the incident wave occurs.

Moreover, when μ is approximately unity, equation (1.15) takes the form

$$\kappa = \frac{e^2}{2\varepsilon_0 mc} \frac{N\nu}{\nu^2 + (\omega \pm \omega_L)^2} \tag{1.21}$$

For cases when $\nu^2 << (\omega \pm \omega_L)^2$, the total non-deviative absorption may then be written as

$$\left(\int \kappa ds\right)_{\mu=1} = \frac{e^2}{2\varepsilon_o mc} \cdot \frac{1}{(\omega \pm \omega_L)^2} \cdot \int N\nu ds. \qquad (1.22)$$

From this expression, it is evident that the non-deviative type of absorption will usually occur in regions where the product Nv is large, which is the case in the D-region.

During the daytime, the non-deviative absorption is usually much greater than the deviative absorption at vertical incidence, except for frequencies near the critical penetration values. At night, however, the deviative absorption is the dominant source of attenuation and prevents the nighttime total absorption from falling below approximately 0.3 nepers. Studies of the non-deviative absorption at night, therefore, are usually made using oblique incidence propagation.

2. THE PULSE REFLECTION METHOD OF MEASURING IONOSPHERIC ABSORPTION

2.1 General Theory

There are a number of different methods that may be employed to measure ionospheric absorption. As defined for the IQSY (1963), these methods can be considered as falling into essentially one of the following main groups:

(i) Measurement of the amplitudes of pulses reflected from the ionosphere.
(ii) Measurement of the absorption of extra-terrestrial radio noise.
(iii) Measurement of the field strength of sky wave signals at short distance and oblique incidence on frequencies suitable for obtaining absorption data.

Since this report is primarily concerned with the first of these techniques, the pulse reflection method shall be the only one discussed here.

It has become common practice to express the experimental measurements of ionospheric absorption in terms of the apparent reflection coefficient ρ. This parameter is defined as

$$\rho = I/I'_o \qquad (2.1)$$

where I is the amplitude of a wave which has been reflected once from the ionosphere and I'_o is the amplitude of the wave which would have been observed in the absence of any absorption, as was previously discussed.

The total ionospheric absorption may then be conveniently written as

$$\int \kappa ds = -\ln \rho \qquad (2.2)$$

In practice, the absorption is usually measured in terms of a loss in decibels, L, where

$$L = -20 \log \rho = -8.686 \ln \rho \qquad (2.3)$$

where log represents the logarithm to the base 10. Thus the measurement of ionospheric absorption consists essentially in experimentally determining the value of **log** p.

If there is no absorption present, the amplitude I of a wave reflected at vertical incidence from a virtual height h' is given by

$$Ih' = I_o h_o \tag{2.4}$$

where I_o is the amplitude which would have been received after reflection **from** a standard height h_o, assuming that h_o is large compared to the wavelength of the operating frequency. Hence, when absorption is present, the amplitude of the first reflection I_1 may be expressed as

$$I_1 h' = \rho I_o h_o = \rho G \tag{2.5}$$

where G may be regarded **as a** calibration constant equal to $I_o h_o$. Similarly, the second-order reflection I_2 can be given by

$$2I_2 h' = \rho\rho_g I_1 h' = \rho^2 \rho_g G \tag{2.6}$$

where ρ_g is the apparent reflection coefficient of the ground. Extending this idea still further, the nth-order reflection may be expressed as

$$nI_n h' = p^n \rho_g^{n-1} e. \tag{2.7}$$

Therefore, when G is known, the value of ρ can be determined from the simultaneous measurement of the virtual height h' and the amplitude of the first-order echo [equation (2.5)]. In general, there are essentially two methods of determining the calibration constant G and, therefore, the apparent

reflection coefficient ρ. The one involves the use of multiple reflections or echoes, whereas the other involves a study of the time-variation of one single echo.

2.2 Determination of Absorption by Use of Multiple Echoes

When multiple reflections are present, the comparison of the amplitudes of the various echoes observed can be used to determine the product $\rho\rho_g$ and the quotient G/ρ_g. Thus, combining equations (2.5) and (2.7), the expression for $\rho\rho_g$ may be written as

$$(\rho\rho_g)^{n-1} = n(I_n/I_1). \tag{2.8}$$

Similarly, for the value of G/ρ_g, this equation may be expressed as

$$G/\rho_g = I_1 h'/\rho\rho_g. \tag{2.9}$$

From these expressions, it is readily apparent that G, p, and hence L may be determined only if the value of the ground reflection coefficient ρ_g can be evaluated.

Perhaps the simplest method of obtaining a reasonable value of ρ_g is to consult a table or map of electrical constants of the ground for a given geographical location (e.g. Jordan, 1950). An alternate method would consist in an experimental approach based on the assumption that the total absorption at night, for frequencies much less than the critical frequency, is relatively small. This would be the case when a large number of reflections are present, thus indicating a relatively small amount of absorption.

The value of the apparent reflection coefficient p may then be assumed to be unity and all residual losses may be attributed to ground losses, The

ground reflection coefficient ρ_g is then determined by use of equation (2.8). It should be mentioned that the most accurate value of ρ_g can be obtained by use of higher order reflections (Piggott, et al., 1957); the higher the order of reflection, the greater the accuracy. Moreover, the most accurate values of the calibration constant G are usually obtained at night when the product $\rho\rho_g$ is relatively large.

Having determined the values of G and ρ_g, the amount of ionospheric absorption L in decibels may then be evaluated by expressing equation (2.5) in the form

$$L = 20 \log G - 20 \log (I_1 h'). \tag{2.10}$$

When multiple reflections are present, L may be found using

$$L = \tfrac{1}{2} [20 \log G + 20 \log \rho_g - 20 \log (2I_2 h')] \tag{2.11}$$

for a second-order echo, or

$$L - 20 \log \rho_g = \frac{1}{n-1} [20 \log (nI_n/I_1)] \tag{2.12}$$

for an nth-order echo (n>2). Generally speaking, when the absorption is small, the over-all accuracy of this method is considerably improved by use of higher-order echoes. In practice, moreover, the highest-order reflection observable is usually selected for this particular measurement.

2.3 Determination of Absorption by Use of a Single Echo

If it is possible to measure only a single reflection, the determination of ionospheric absorption must be based on a study of the time-variation of this echo. If the amplitude I of the echo at time t_1 has an apparent reflection

coefficient ρ_1, and at time t_2 a reflection coefficient of ρ_2, equation (2.5) may be written as

$$(I_1 h')_{t_1} / (I_1 h')_{t_2} = \rho_1 / \rho_2 \tag{2.13}$$

if the echo observed is the first-order reflection. Similarly, for an nth-order echo, equation (2.7') may be expressed as

$$(I_n h')_{t_1} / (I_n h')_{t_2} = (\rho_1 / \rho_2)^n. \tag{2.14}$$

Equation **(2.13)** is generally used in this method, whereas equation (2.14) would only be employed if there were severe "splitting" or distortion of the first-order reflection.

If the time t_2 is made sufficiently small to be considered negligible, the ratio ρ_1/ρ_2 may then be assumed to be ρ_1. The loss L at time t_1 due to absorption of the transmitted wave is then given as

$$L = 20 \log (I_1 h')_{t_2} - 20 \log (I_1 h')_{t_1}. \tag{2.15}$$

Moreover, if ρ_2 is assumed to be approximately unity when $t = t_2$, the value of $I_1 h'$ is then equal to $I_o h_o$, or the calibration constant G. For this case, equation (2.13) may be conveniently expressed as

$$L = 20 \log G - 20 \log (I_1 h'). \tag{2.16}$$

Therefore, if it is possible to measure G when conditions are such that $\rho = 1$, the value of ionospheric absorption L may be found for any time t.

The only advantages of using the single echo method, rather than the multiple reflection technique, are that it is much simpler and does not

require the determination of the apparent ground calibration coefficient p_g. However, in practice, the multiple reflection method is preferred, especially in cases where the absorption is relatively small.

2.4 Practical Measurement Techniques

In general, the practical techniques involved in measuring ionospheric absorption consist simply in the analysis of the radio wave reflections of a number of consecutively transmitted pulses. The three main methods employed at the present time are:

(i) Constant-output technique.
(ii) Constant-gain technique.
(iii) Quasi-logarithmic technique.

The experimental results obtained by each of these methods are comparable in accuracy, providing, of course, that adequate precautions have been taken to eliminate the errors inherent in each technique,

In the constant-output technique, the receiver output is displayed on an oscilloscope and the magnitude of the desired reflection is maintained at a constant level by means of the calibrated receiver gain control. The gain control setting is recorded at convenient intervals; each setting corresponding to a certain amount of attenuation in decibels. Calibration curves then permit the translation of these relative values into the actual reflected signal amplitudes.

In the constant-gain technique, the receiver gain is maintained at a constant value while the average amplitude of a given echo is determined from the oscilloscope trace. Once again, recordings of the average amplitude are made at suitable intervals and the relative amount of attenuation or absorption

of the selected echo is determined. It is important to note that both the constant-output and the constant-gain techniques are visual methods, and hence, greatly susceptible to human error.

The quasi-logarithmic technique has been developed primarily to eliminate these observational errors through the automatic measurements of amplitude and of absorption. Echo-selecting gates and integrators are usually used so that fast fading is smoothed out and the slow variations of the different echo orders can easily be determined. The records enable the median log amplitudes to be found, It should also be mentioned that preci'se design and calibration procedures are extremely important to the successful application of this technique, since any variation in the system parameters will subsequently result in a variation of the recorded values.

2.5 Influence of Non-Dissipative Phenomena

It is evident from the preceding discussion that the measurement of ionospheric absorption is dependent primarily upon the measurement of the variations in the amplitude of radio waves. The problem, however, is somewhat more complicated, since absorption is not the only factor affecting the amplitudes of radio waves in the ionosphere. Other factors due to non-dissipative processes also have an effect and, hence, may introduce error into the measurement.

It is necessary, therefore, to investigate the influence of non-dissipative phenomena on the amplitude of radio waves and to examine possible methods of minimizing their effect. The main non-dissipative phenomena (Piggott, et al., 1957) affecting radio wave propagation are:

(i) Polarization.

(ii) Dispersion.

(iii) Spatial attenuation.

(iv) Scattering and partial reflection.

(v) Fading.

From magneto-ionic theory, it can be shown that an electromagnetic wave of arbitrary polarization will excite two characteristic components, the ordinary wave and the extraordinary wave, upon incidence with the ionosphere. The amplitudes, polarizations, and propagation paths of these two excited waves, moreover, will be independent of each other, except in a few special cases, The ionospheric characteristie polarizations, however, seldom change significantly with time. Therefore, for absorption studies, it is sufficient to use antenna systems of constant gain and polarization. En practice, balanced plane-polarized antennas are generally used to eliminate the effect of polarization on the measurement of absorption.

It can also be shown that when a pulse ofelectromagnetie energy is transmitted through the ionosphere, the variation of the phase path with frequency will alter the relative phases of the side-band frequencies. Thus the shape of the signal is changed. This phenomenon, known as ionospheric dispersion, is dependent on the total amount of phase shift due to the transmitter, the ionosphere, and the receiver. The effect of dispersion can be minimized quite simply by increasing the transmitted pulse-width until the amplitude of the highest-order reflection is independent of any additional increase in the width of the pulse, At this condition, the effect of ionospheric dispersion is negligible.

Electromagnetic wave theory also predicts that the amplitude of a wave radiated from a point source in free space will vary inversely with the distance.. from the source. A similar law applies to the spatial attenuation of radio

waves reflected from the ionosphere at vertical incidence, The amplitude of the wave will vary inversely with the path length, which is equal to twice the virtual height of reflection at vertical incidence. While this result is strictly true only if the effect of the earth's magnetic field is neglected, the errors introduced into the measurement of absorption by spatial attenuation are, in practice, quite small.

Scattered reflections from large, abnormally dense ionization clouds are another source of radio wave attenuation in the ionosphere, At vertical incidence, the normally reflected wave may be seriously attenuated by the presence of these irregularities, thus introducing serious error into absorption measurements. Partial-reflection phenomena from the E_s-layer often occur on frequencies which are slightly above the critical frequency of the E-layer and, hence, the amplitude of the F-echo is considerably decreased as a result of these losses. It should be mentioned that there is no method of eliminating the effect of these partial reflections, unless, of course, the total loss due to this scattering can be evaluated. In general, it can be said that useful absorption data cannot be obtained when severe scattering exists. Since partial reflections are significantly present in high latitudes, this seriously restricts the determination of absorption in this region.

The final and, perhaps, most important non-dissipative phenomenon is fading. Fading may be defined as the variation in the pulse amplitude of a signal due to random irregularities in the ionization density. The sate of fadfng, moreover, depends upon the relative change in the phase paths of two superimposed waves and the depth of fading depends upon the difference in the amplitudes of the modes. In general, there are two types of fading: fast fading, where the average fading

period is between one second and one minute; and slow fading, where the average period may lie between 5 and 50 minutes.

The fading of multiply-reflected signals, moreover, is usually faster and deeper than that of the first-order reflection. Slow fading is almost always present, but is more severe at night. In practice, it is desirable to select a sampling period that will include as many fading periods as possible, the maximum interval being limited by the diurnal variation in the rate of ionization density. A sampling period of between 10 and 20 minutes is generally used. The theory of fading, however, is somewhat more complex than the treatment given here, and much work has been done in the probability and statistics of this phenomena. A comprehensive study has been made by Piggott, et al. (1957).

3. THE ABSORPTION MEASUREMENT TECHNIQUE USED AT THE UNIVERSITY OF ILLINOIS

3.1 General Description

The Aeronomy Laboratory of the University of Illinois has undertaken a program of investigation of the lower regions of the ionosphere by use of rockets and ground-based sounding techniques, The experiments are performed at the NASA launch site at Wallops Island, Virginia, and the combination of the rocket data and that obtained by conventional sounding methods are giving a new insight into the behavior of the ionosphere.

The purpose of this chapter is to describe the sounding system presently being used at Wallops Island to obtain absorption data. The system, shown in Figure 3.1, operates on a frequency of 3.030 Mc/s with an effective radiated power of approximately 50,000 watts.

In addition to the measurement of ionospheric absorption, the equipment was also designed to be capable of obtaining partial reflection data. However, since the present work is not concerned with this particular type of measurement, only the operation of the system pertaining to the determination of absorption will be discussed in the following sections.

3.2 Transmitting Equipment

The transmitter used in this experiment is essentially a conventional pulsed transmitter with a carrier frequency of 3.030 Mc/s. Only a general description will be given here, since the details of this equipment will soon be available in a published report by Henry (1965). The transmitter block diagram is shown in Figure 3.2.

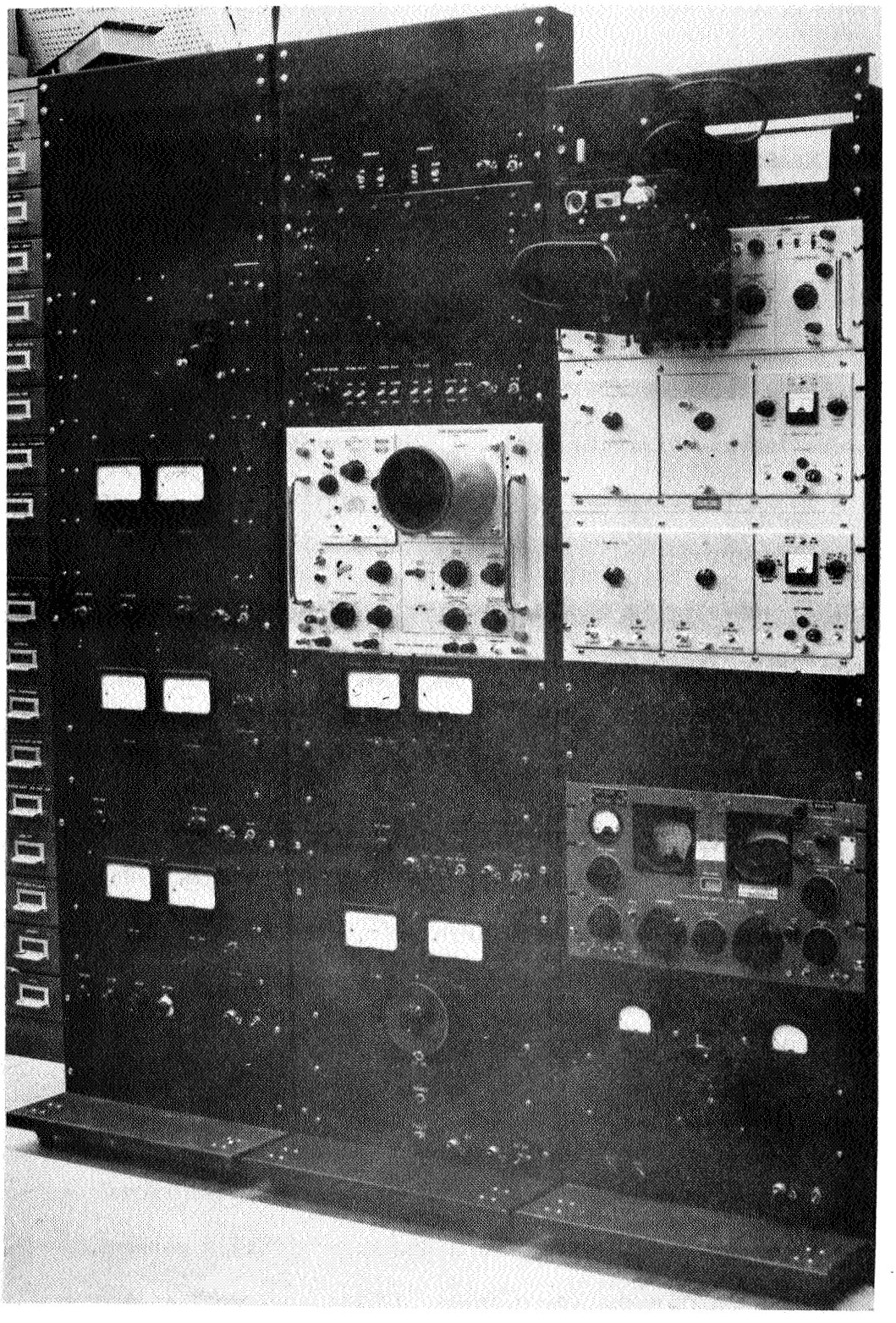

Figure **3.1** The 50 kw ionospheric sounding system used **for** absorption measurements.

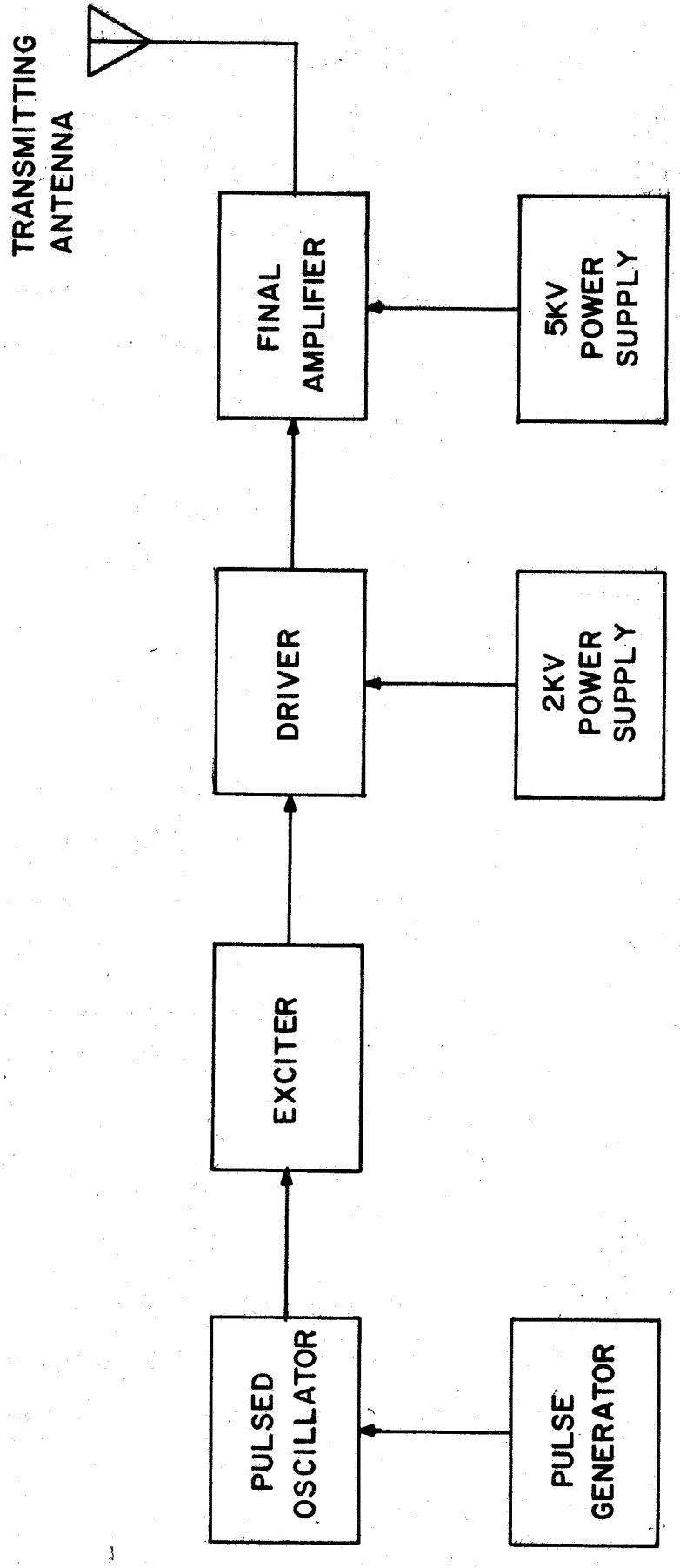

Figure M 2 Block diagram of the transmitter.

The pulse generator, which is synchronized to the line frequency of 60 c/s, generates positive pulses at a fixed repetition rate, which may be selected as either 0.5, 1.0, 2.0, or 5.0 pulses/sec. The width of this pulse, moreover, may be varied from 30 to 100 microseconds by use of an adjustable delay multivibrator. For normal operation, a pulse width of approximately 50 microseconds is generally selected. This pulse, in turn, is used to gate a crystal-controlled oscillator operating at 3.030 Mc/s, thus producing a 50 microsecond burst of the carrier frequency.

The output of the pulsed oscillator is then applied to the exciter, which consists of two stages of amplification; the first stage employing a type 12AU7 tube and the second stage a type 6AG7. The driver is essentially a tuned power amplifier consisting of two type 7094A tubes operating in the conventional push-pull configuration. The plate voltage of this stage, moreover, is supplied by the 2kv power supply. The output tubes of the final amplifier are two RCA type 7214, once again operating in the push-pull mode. The plate voltage is supplied by the 5kv power supply and the tubes are air-cooled to prevent overheating.

As a relative indication of the power capabilities of this system, the peak output power of each unit can be given as follows:

(i) Pulsed oscillator : 2 watts
(ii) Exciter : 20 watts
(iii) Driver : 3.5 kw
(iv) Final amplifier : 50 kw

A peak output power of 50 kw is more than sufficient for absorption measurements; depending on existing noise conditions, an effective output power of 1 to 10 kw will usually suffice for this type of experiment. The selection of

a 50 kw system was dictated primarily by its necessity in the study of partial reflections; however, the higher power has facilitated calibration of the system using multiple reflections under a wider range of ionospheric conditions than would otherwise have proved possible.

3.3 Receiving Equipment

A general description of the receiving equipment will be given here, since the details are once again discussed in the report by Henry (1965). The receiver block diagram is shown in Figure 3.3, and consists essentially of an RF amplification stage, a local oscillator, a mixer, an IF amplification stage, and a detector, all of which have been suitably designed for pulse reception,

The receiver has an input impedance of 50 ohms and a first stage noise figure of approximately 2.5 db at 3,030 Mc/s. The RF section, moreover, has a manual gain control with a maximum effective range of 30 db. The local oscillator frequency has been selected as 8.030 Mc/s and is crystal-controlled. The output of the mixer, therefore, is the intermediate frequency of 5.000 Mc/s, the difference between the local oscillator and carrier frequencies, The IF section of the receiver also bas a manual gain control and consists of four stages of amplification with a maximum gain of 25 db/stage

The receiver, therefore, has a maximum gain of 160 db, with a gain control dynamic range of approximately 80 db. The overall bandwidth of the receiver, measured between the 3 db points, is approximately 35 kc/s. This bandwidth is necessary to eliminate any distortion of the pulse shape by the tuned circuits. A standard oscilloscope, synchronized with the output of the pulse generator, is employed to display the return signal.

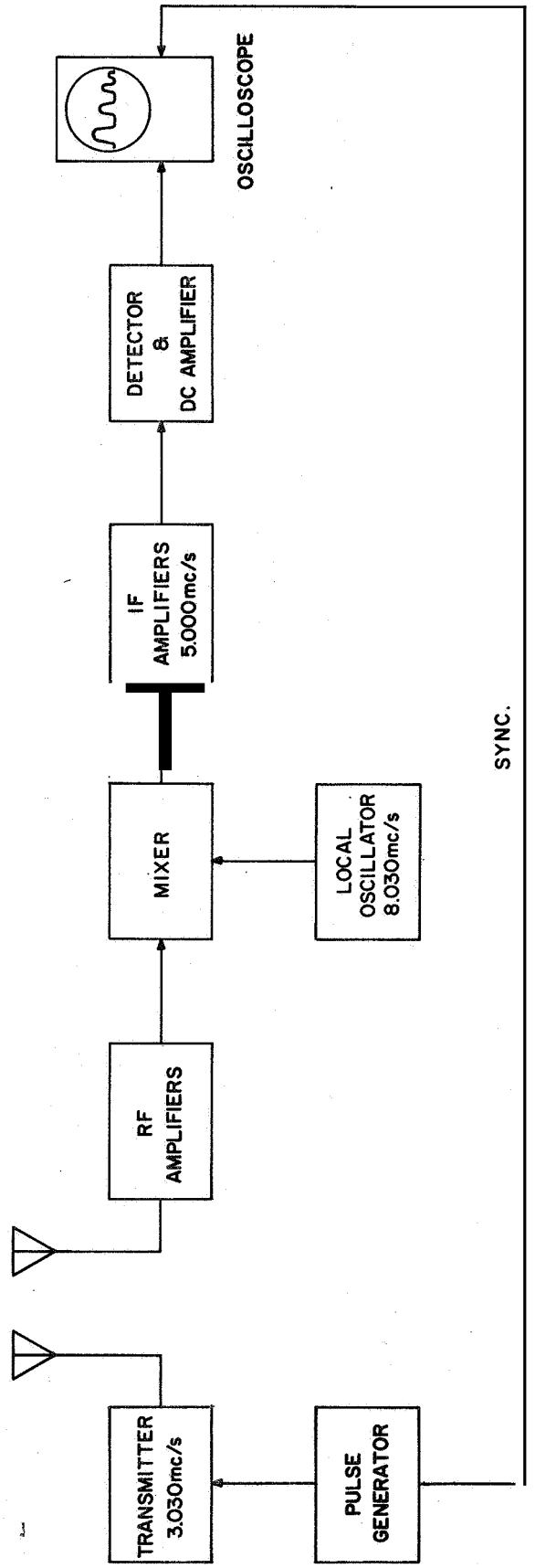

Figure 3.3 Block diagram of the receiver

Use of the automatic recording system described in Chapter 4 necessitated a modification of the receiver; the manual IF gain control was replaced with an external AGC circuit. The AGC characteristic of the receiver, moreover, had to be approximately logarithmic, since this property is essential for the operation of the automatic recording system, The IF amplifier stage with the AGC circuit is shown in Figure 3.4 and the corresponding AGC characteristic curve is shown in Figure 3.5. With the application of an external AGC voltage of 5 to 11 volts, the IF receiver gain may be varied over a 40 db range.

3.4 Antenna System

The transmitting and receiving antennas at Wallops Island are identical four dipole box arrays. The transmitting antenna is a conventional array consisting of two parallel sets of delta-matched half wave dipoles spaced a half wavelength apart and is designed to transmit circularly polarized waves at a frequency of 3.030 Mc/s. The receiving antenna is a conventional folded dipole array, once again consisting of two parallel sets of half wave dipoles spaced a half wavelength apart, The geometry of the antenna system is shown in Figure 3.6.

The transmitting antenna is a 470 ohm open wire array, whereas 300 ohm Twin-Lead is used for the receiving antenna. The antennas are elevated at a height of approximately a quarter wavelength above the ground, The arrays may be used to transmit and receive either the ordinary or extraordinary radio wave modes.

3.5 Determination of Absorption

The absorption measurement technique presently being used by the Aeronomy Laboratory is essentially the constant-gain technique described in Chapter 2.

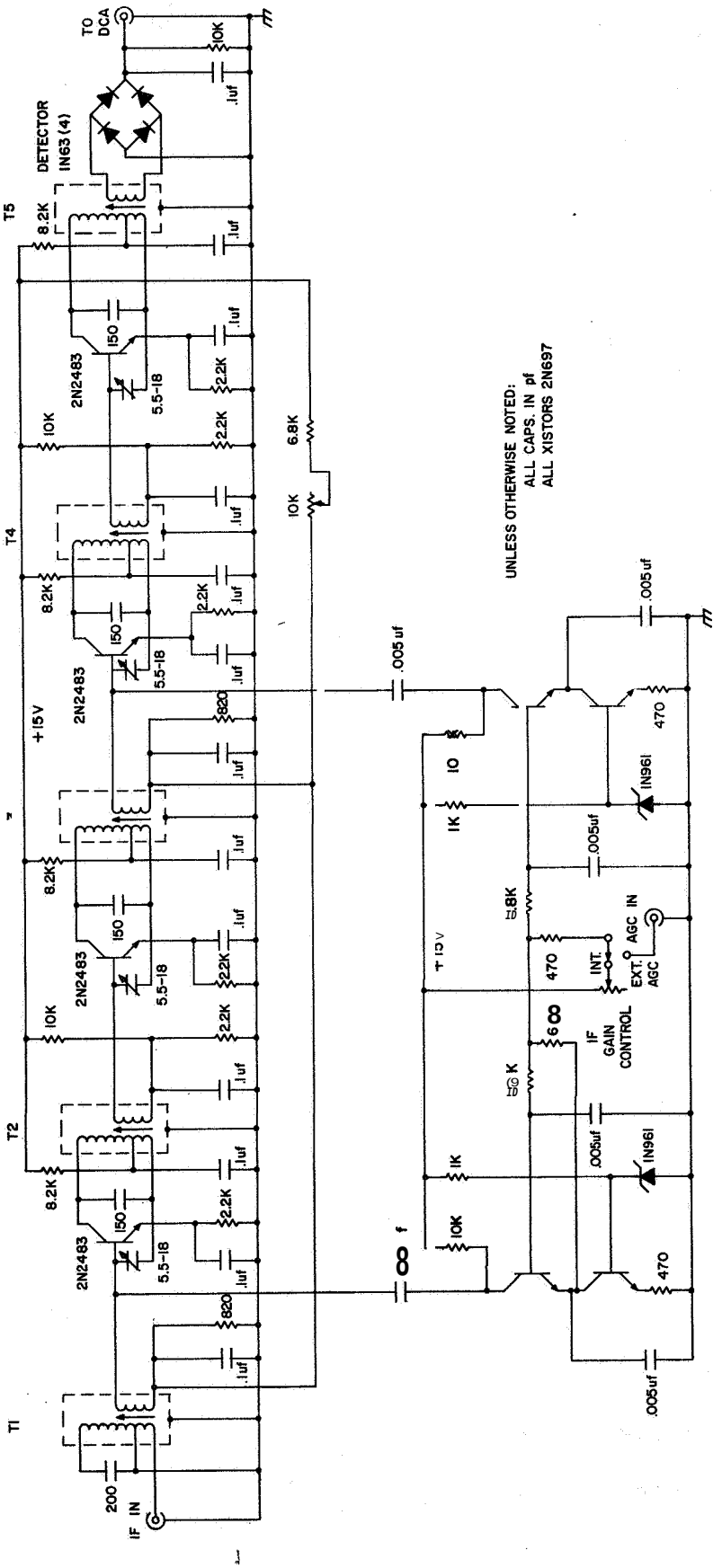

Figure 3 4 Schematic diagram of IF amplification stage, detector, and external AGC circuit.

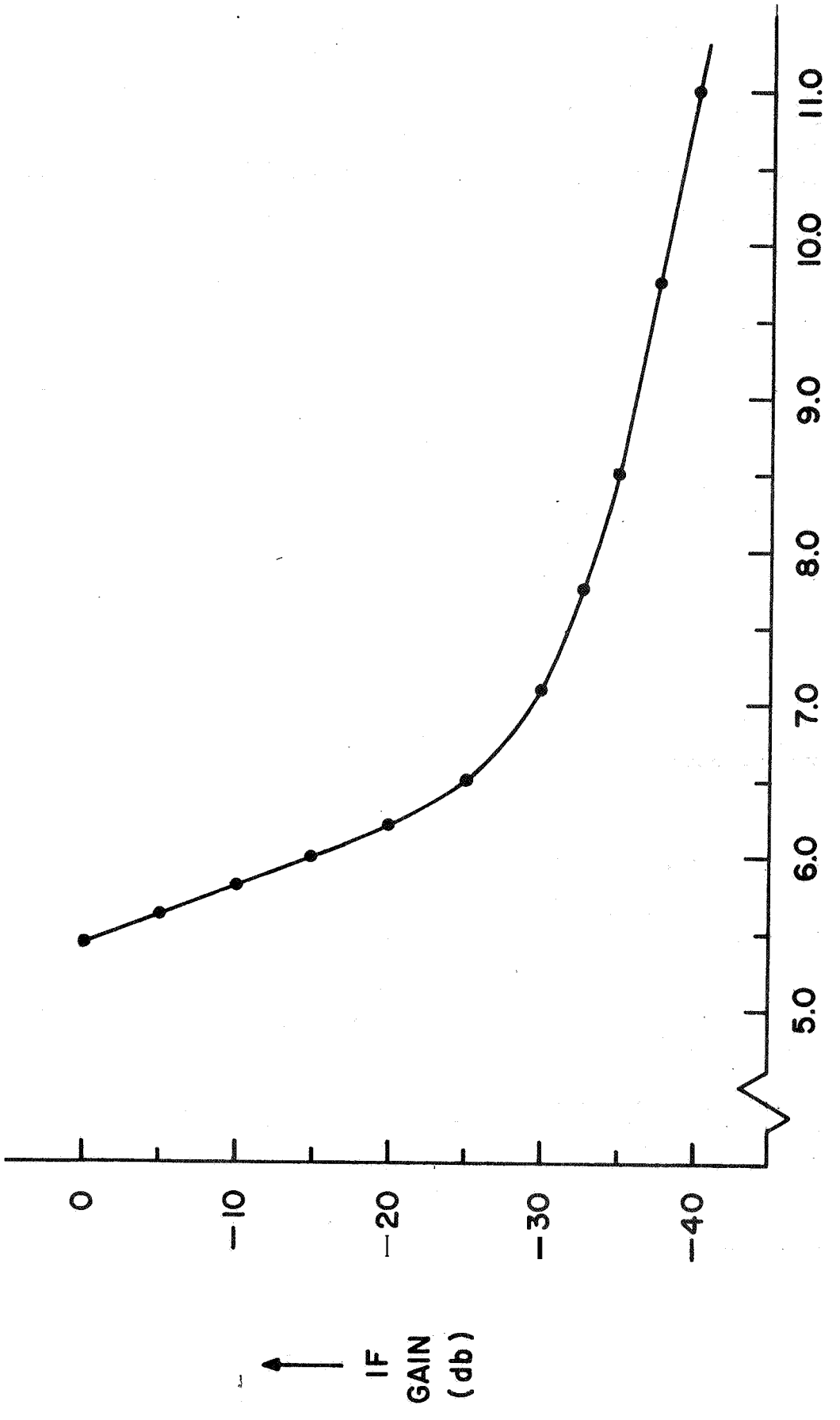

Figure 3.5 AGC characteristic of the receiver

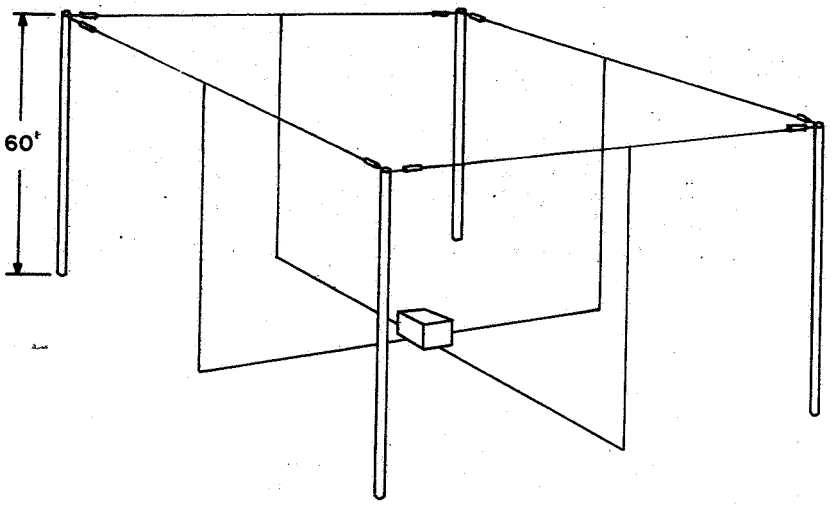

A

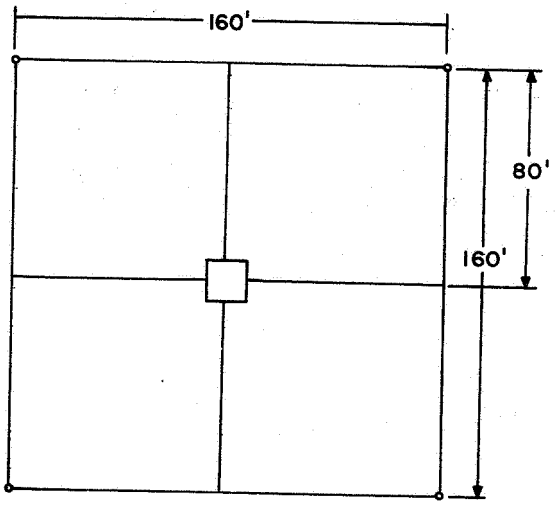

B

TRANSMITTER:
DELTA-MATCHED DIPOLE

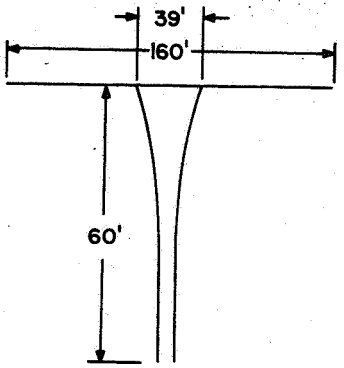

C

RECEIVER:
FOLDED DIPOLE

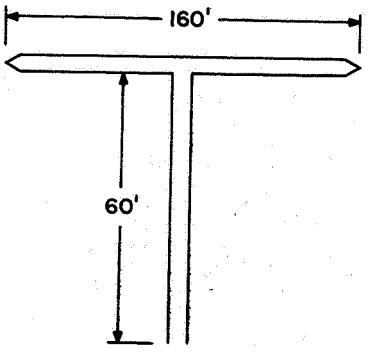

D

Figure 3.6 T antenna system at Wallops Island, Virginia: (A) general configuration of transmitting and r eiving arrays; (B) top view of arrays; (C) transmitter dipole; (D) receiver dipole.

The receiver gain is adjusted to a suitable value to display the desired echo on the oscilloscope screen. The return signals are then photographed by use of a Beattie-Coleman 35 mm oscillotron camera system which is synchronized with the output of the pulse generator, After processing, the film is displayed on a Recordak film reader and the pertinent information is measured directly off the trace.

The following procedure has been adopted for the measurement of absorption:

(i) A receiver calibration curve is obtained by applying a known signal to the receiver input and measuring the output voltage for various gain control settings. The voltage gain is then converted to decibel gain and a curve of receiver attenuation versus gain control setting is plotted.

(ii) The transmitter is tuned for maximum power output and the receiver gain is adjusted to display the desired echo on the oscilloscope. The RF and IF gain control settings are recorded, as well as the film frame number. The camera system has an internal clock and, therefore, the time of day is recorded directly on the film.

(iii) The pulse repetition rate of the transmitter is seleeted at 0.5 pulses/sec, thus giving an average of 30 recordings/minute. A 10 minute interval constitutes one sampling period.

In addition to the above procedure, the calibration constants G and p_g are evaluated at night using the multiple refleetions technique described in Chapter 2. The amplitudes of the first- and second-order echoes are measured and the calibration constants are determined by use of equations (2.8) and (2.9). These values may then be used to calculate the daytime absorption level.

The following procedure is presently being used to calculate the absorption value L:

(i) The recorded gain control settings are converted into the corresponding attenuation values in decibels.

(ii) The relative amplitudes of the echo under study are measured directly from the film reader trace, as well as the virtual height, h', at which the echo occurs.

(iii) The relative echo amplitudes are converted into the corresponding attenuation values by use of the receiver calibration curve.

(iv) The average values of the amplitude of the echo and the virtual height are calculated for the 10 minute sample.

(v) The average values of amplitude and virtual height obtained in (iv) and the value of the calibration constant G obtained at night are substituted into equation (2.10) to give the absorption value L for the 10 minute interval.

This procedure is in accord with the recommendations for absorption measurements proposed for the IQSY (1963).

4. THE AUTOMATIC RECORDING SYSTEM

4.1 Purpose of the System

The manual method described in Chapter 3 to analyze absorption data involves a great amount of tedious and repetitious work. Specifically, the method presently being used by the Aeronomy Laboratory has the following disadvantages:

(i) The system requires continual monitoring by an operator, who must frequently adjust the receiver gain controls and record the various settings.

(ii) The manual method of measuring the amplitudes of the reflections from the film reader is a tedious process and subject to observational errors.

(iii) The mathematieal calculations involved in determining the absorption value L are rather time-.consuming and, therefore, expensive.

Since the study of the behavior of the ionosphere by the absorption measurement technique depends primarily on the daily variation of the absorption level, it is evident that the present system would not be feasible for a long-term study. The purpose of the proposed system, therefore, is to automatically measure the amount of ionospheric absorption and provide a permanent record for further analysis. Clearly, a system of this type should incorporate the fallowing features:

(i) An automatic averaging device which translates a series of consecutive readings of the reflection amplitude into some median value.

(ii) A system capable of automatically measuring the virtual height of reflection of the echo, thus giving a relative indication of how the refleetion layer is varying.

(iii) A recording device which gives an immediate indication of the average absorption level.

(iv) A recording device capable of storing the absorption and virtual height data in a form suitable for further analysis on a computer.

Moreover, the system should be designed so as to eliminate the necessity of continual monitoring by an operator. With these criteria in mind, it is now possible to discuss the proposed automatic recording system and to see how it satisfies each of the above-mentioned requirements.

4.2 General Description

The proposed automatic recording system for the determination of ionospheric absorption is based on the quasi-logarithmic technique briefly discussed in Chapter 2. The system measures the mean amplitudes of the desired reflections and employs a feedback system, where the signal applied to the receiver AGC line is linearly proportional to the difference between the mean echo amplitude and a fixed reference voltage, Since the receiver AGC characteristics are approximately logarithmic (Chapter 3), the AGC voltage is therefore proportional to the absorption level.

Only a block diagram description of the automatic recording system will be given here, since the details are treated in the following chapters, The block diagram of the proposed system is shown in Figure 4.1 and the experimental equipment is shown in Figure 4.2.

The signal from the pulse generator is applied simultaneously to the transmitter and the gate generator. The latter circuit provides a gating pulse at a time determined by the particular echo to be measured. This pulse is then gated with the return signal from the receiver and the resultant output of the echo selector is the desired reflection where all other echoes have been suppressed.

This signal is then applied to an integrator circuit with a time constant of approximately 50 seconds. The resultant output, therefore, is a slowly varying dc level, which is proportional to the mean echo amplitude. A dc

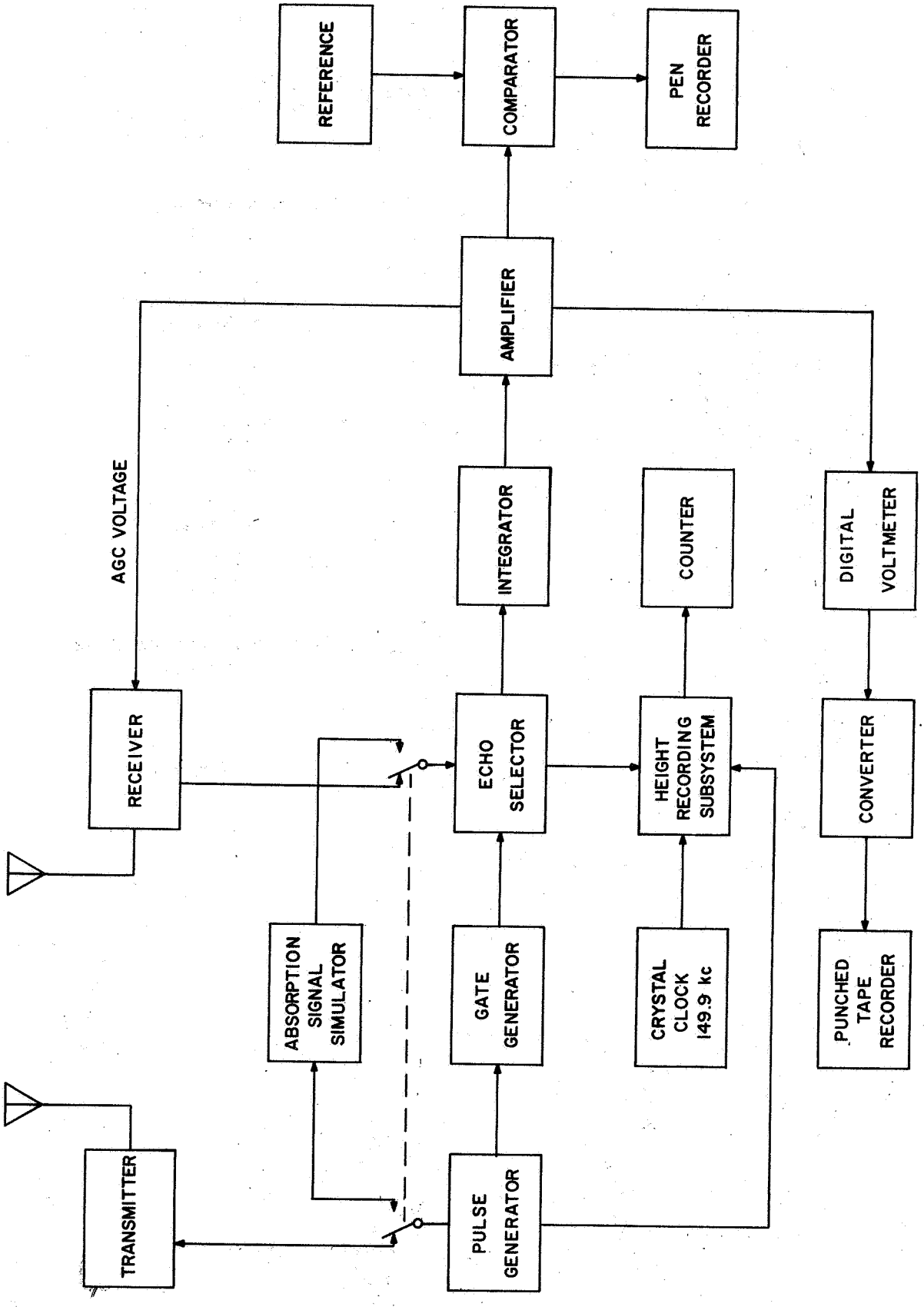

Figure 4.1 Block diagram of the automatic recording system

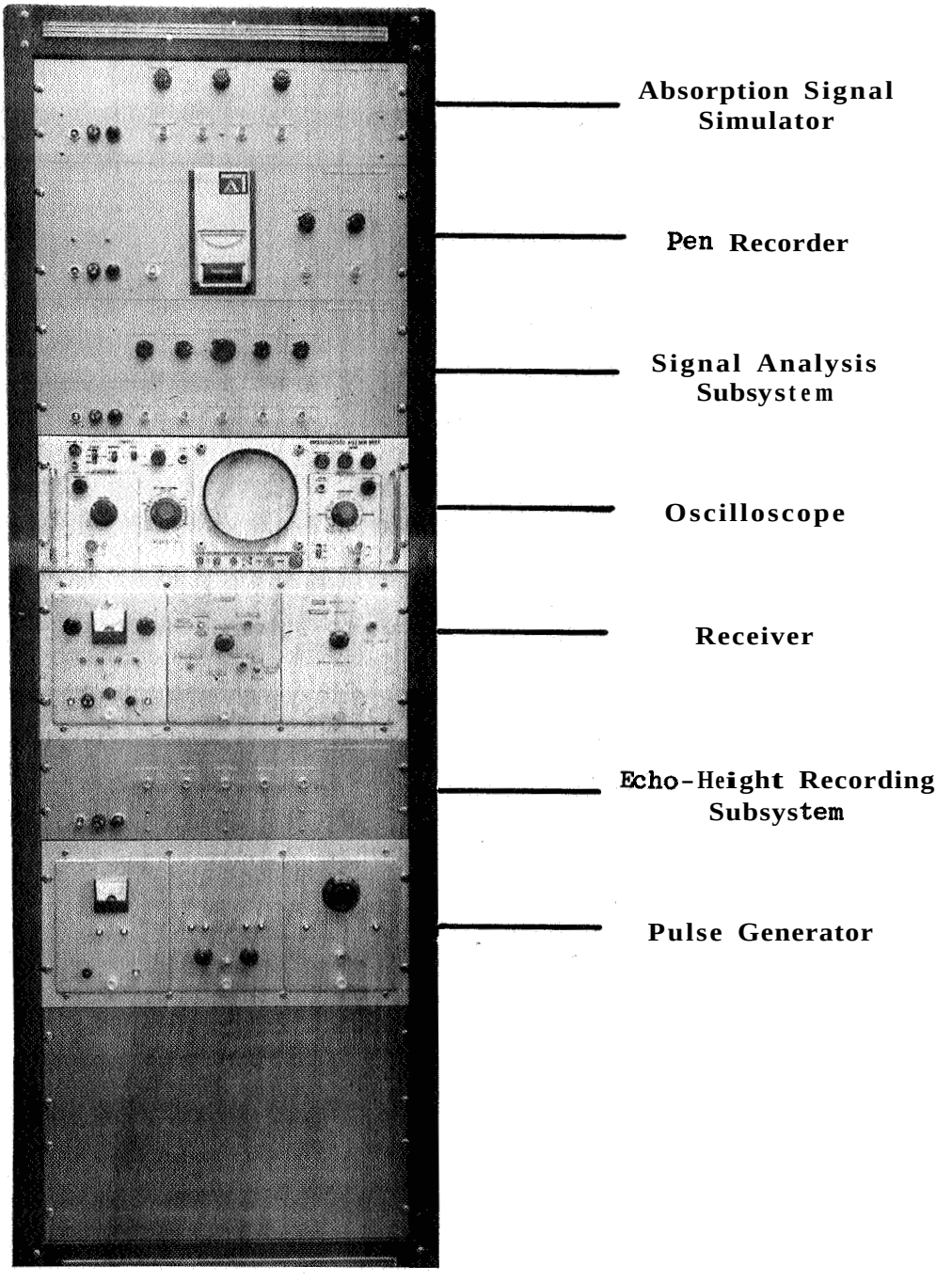

Figure 4.2 The automatic recording system.

amplifier is used to provide the necessary AGC voltage for the receiver, thus completing the closed-loop system.

The output of the amplifier is applied to a comparator circuit and the difference between this voltage and a calibrated reference voltage is recorded on pen recorder, thus giving an immediate indication of the absorption level. Since the variation in ionospheric absorption is useful in obtaining electron density profiles of the ionosphere (see Chapter 8), an alternate method of recording the absorption level will be employed. The output of the de amplifier will be measured on a digital voltmeter and permanently recorded on punched-tape by a Tally recorder. This data will then be fed into a computer, which has been suitably programmed, and an electron density profile of the ionosphere may be automatically calculated.

In addition to the signal analysis part of the system (see Chapter 6), the virtual height at which the selected echo occurs is also automatically determined. The output of the pulse generator is used to set a bistable multivibrator, which remains at a fixed output voltage until it is reset by the output of the echo selector. The output of the multivibrator is then used to gate a crystal-eontrolled square wave generator operating at a frequency of 149.900 kc/s. This particular operating frequency was selected in order that one cycle of this frequency was equivalent to 1 km of height (see Chapter 7). The number of cycles recorded on a counter is then a direct indication of the virtual height of reflection in kilometers.

For laboratory test purposes, it was also necessary to simulate the anticipated' absorption signal, Thus, an absorption signal simulator was designed to replace the transmitter and receiver as shown in Figure 4.1. This unit

simply provides a number of simulated reflections from the ionosphere at the expected intervals and will be described in detail in Chapter 5.

4.3 Practical Design Considerations

It is well known that radio wave reflections from the ionosphere exhibit a wide range of characteristics depending on such factors as geographical location, time of day, time of year, and solar activity. Hence, there are a number of practical considerations that must be taken into account in the design of a system capable of measuring these reflections. Essentially, the system must be carefully designed to eliminate apparent amplitude variations due to component variations in the system itself. Moreover, the system must contain a sufficient number of controls to obtain useful absorption data under any given circumstance.

En the design of the gate generator, it is necessary to provide controls that can vary both the position and width of the gate pulse, in order that all echoes, except the desired reflection, are suppressed. For example, it is a fairly common occurrence for the F-echo to occur at approximately the same apparent height of reflection as the 2E-echo (i.e., an echo that has been reflected twice from the E-layer of the ionosphere). Therefore, it is necessary to adjust the position and width of the gate pulse until the echo under study is included in the gating period, while the other echo is suppressed. Moreover, it is also necessary that the gating period be made long enough, in order that a height-varying echo does not fall outside of the gating period at any time during the sampling interval.

Precise design of the integrator circuit is also important for the successful operation of the automatic recording system, It is necessary that

a linear relationship exist between the integrator output and the product of the pulse width and the pulse amplitude of the input signal. Since in absorption measurements the pulse width remains essentially constant, the output of the integrator will therefore bear a linear relationship to the mean pulse amplitude as required,

Moveover, in order that the integrating capacitor may be able to retain its charge accurately for a long period of time, the capacitor must have low leakage and, hence, must be carefully selected. However, as the charge on the capacitor builds up, even low leakage becomes important, so that long period integration and accurate integration become incompatible. In general, the maximum feasible integration period for accurate measurements is approximately one minute (Jenkins and Ratcliff, **1953).** It is also necessary that the output of the integrator be connected to a coupling stage with a very high input impedance, in order to eliminate any change in the time constant of the integrator by shunting the capacitor with an external load,

Since drift is quite common in dc amplifiers, it is also important that the amplifier be carefully designed to eliminate this effect as much as possible. Moreover, the amplifier must have a sufficiently linear gain control to pravide the required receiver AGC voltage over a wide range of amplitude levels, For example, the amplitude of the 1E-echo is usually much greater than that of the 2E-echo. Hence, in order to provide the necessary AGC voltage, the gain of the amplifier for the 2E-echo measurement must be much greater than that for the 1E-echo measurement.

It should be mentioned that the gate generator, integrator, and dc amplifier circuits are the critical design problems in the automatic recording system, and hence have been treated in great detail, Other design problems exist, however, and will be treated in the following chapters.

5. THE ABSORPTION SIGNAL SIMULATOR

5.1 Purpose of the Signal Simulator

As mentioned in Chapter 4, it was necessary to design and construct a unit to simulate the characteristics of the transmitter and receiver, in order to test the automatic recording system in the laboratory. The purpose of the absorption signal simulator, therefore, is to provide a number of simulated reflections from the ionosphere at intervals where the reflections are most likely to occur.

This unit, moreover, facilitates the design of the other circuits in the automatic recording system. Specifically, it is useful in determining the range of operation of the gate generators and in giving a relative indication of the voltage levels in the system. By varying the position and peak amplitude of a particular simulated echo, the response of the automatie recording system may be determined over a wide range of anticipated ionospheric conditions.

5.2 General Description

The schematic diagram of the absorption signal simulator is shown in Figure 5.1. The output of the pulse generator, which provides synchronization for the entire automatic recording system, is inverted and applied to the base of a unijunction transistor of a sawtooth generator. The negative pulse causes the emitter of the unijunction to conduct. Positive feedback is employed and the circuit oscillates at a frequency determined by the capacitor divider feedback network and by the amount of current injected into the base of the unijunction.

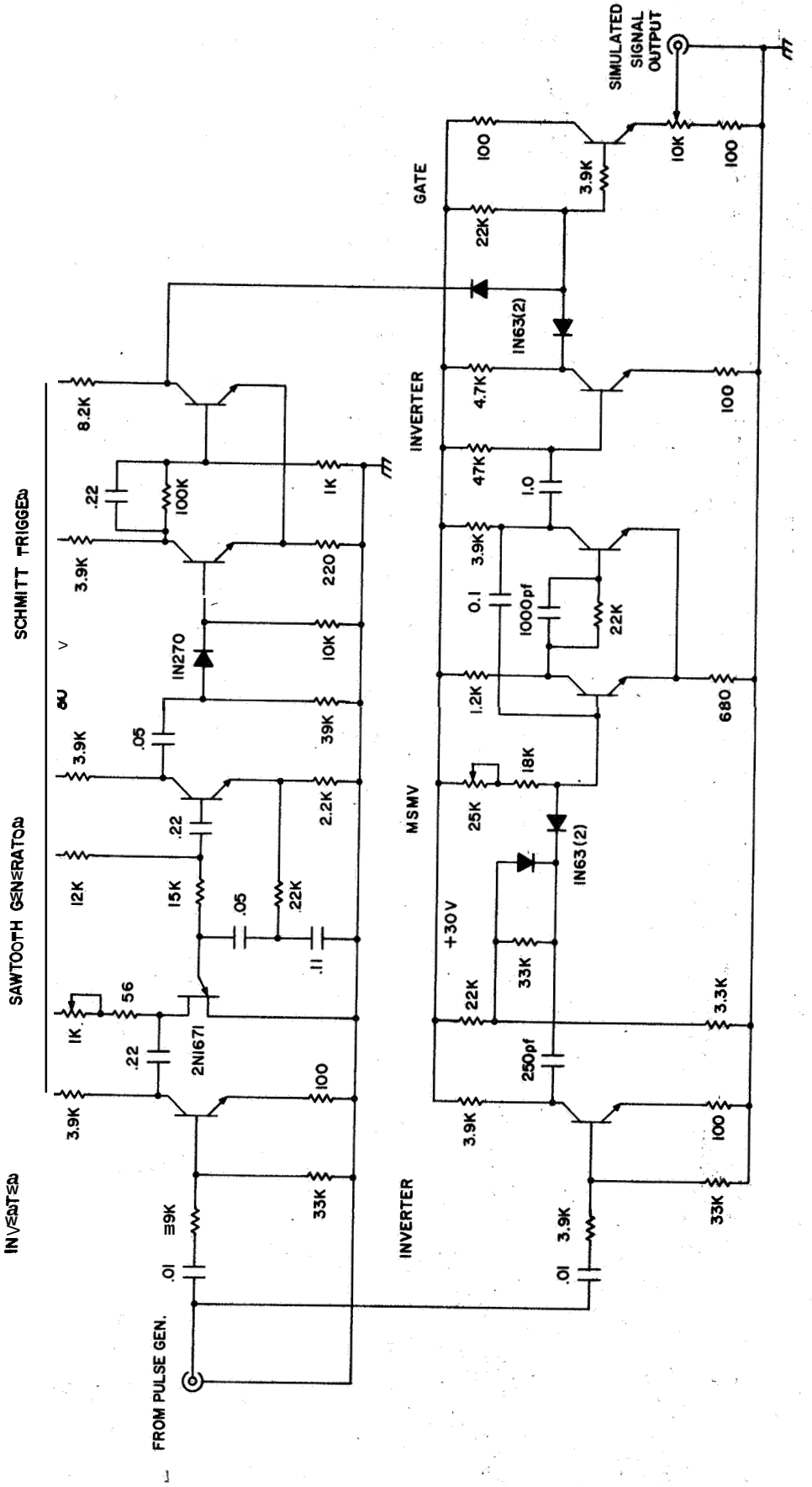

Figure 5.1 Schematic diagram of the absorption signal simulator.

The apparent height at which a radio wave is reflected from the ionosphere is equal to one-half the product of the speed of light and the time required for the wave to travel to the ionosphere and back. Assuming the speed of light as 3×10^5 km/sec, a wave will traverse an apparent distance of 15 km in 0.1 msec. Since the LE-echo usually occurs in the height range from 90 to 150 km, the period of oscillation of the sawtooth generator was selected to lie in the range from 0.6 to 1.0 msec or from 1,667 to 1,000 c/s. This frequency range is obtained by varying the base current of the unijunction transistor.

The output of the sawtooth generator is then applied to a Schmitt trigger which changes the sawtooth waveform into a rectangular pulse; the width of the pulse being determined by the amount of time the output transistor remains in the "off" state. A pulse width of 0.1 msec is selected for normal operation. Any desired width may be obtained by changing the collector-base coupling parameters. The output of the Schmitt trigger, therefore, is a continuous pulse train synchronized with the output of the pulse generator and having a pulse repetition frequency of 1,000 to 1,667 c/s and a pulse width of approximately 0.1 msec.

The output of the gate generator is also applied to a monostable multivibrator (MSMV). The output transistor of the MSMV circuit remains in the "on" state for a time determined by the collector-base coupling network and by the base bias applied to the input transistor, The width of the pulse may be varied from approximately 0.5 to 2.5 msec by changing the base bias on the input transistor. This pulse is then inverted and applied to one input of a conventional "and" gate.

The output of the Sehmitt trigger is fed into the other input of the gate and the gate remains open for a time determined by the time constant of the MSMV. The resultant output of the gate is the number of pulses which lie within the gating period, with all other pulses suppressed. The amplitude of the output pulses may be varied from approximately 1 to 24 volts by selecting the amount of signal desired from the emitter resistor of the output transistor.

Typical waveforms of the absorption signal simulator are shown in Figure 5.2. Figure 5.2a shows the 1E-echo occurring at an apparent height of reflection of 105 km (0.7 msee time delay) and the 2E-echo occurring at an apparent height of 210 km (1.4 msee time delay). Figure 5.2b depiets essentially the same situation, exeept that the amplitudes of the echoes are somewhat less than in the previous ease, If multiple reflections are to be studied, Figure 5.2c shows the case where three echoes are present: the 1E-echo occurring at 90 km: the 2E-echo occurring at 180 km; and the 3E-echo occurring at 270 km. Any number of echoes may be obtained by changing the width of the gating pulse. Moreover, the position of the 2E- or 3E-echo may be adjusted to a suitable value to simulate a refleetion from the F-layer of the ionosphere.

5.3 Practical Design Considerations

It is evident from Figure 5.2 that the pulses generated by the absorption signal simulator are an imperfect representation of received reflections from the ionosphere; the signals obtained by eonventional sounding techniques are usually Gaussian-shaped půlses. Moreover, the various eehoes are not of constant amplitude, but vary greatly depending on existing conditions. The simulated signals, however, are sufficient for laboratory test purposes,

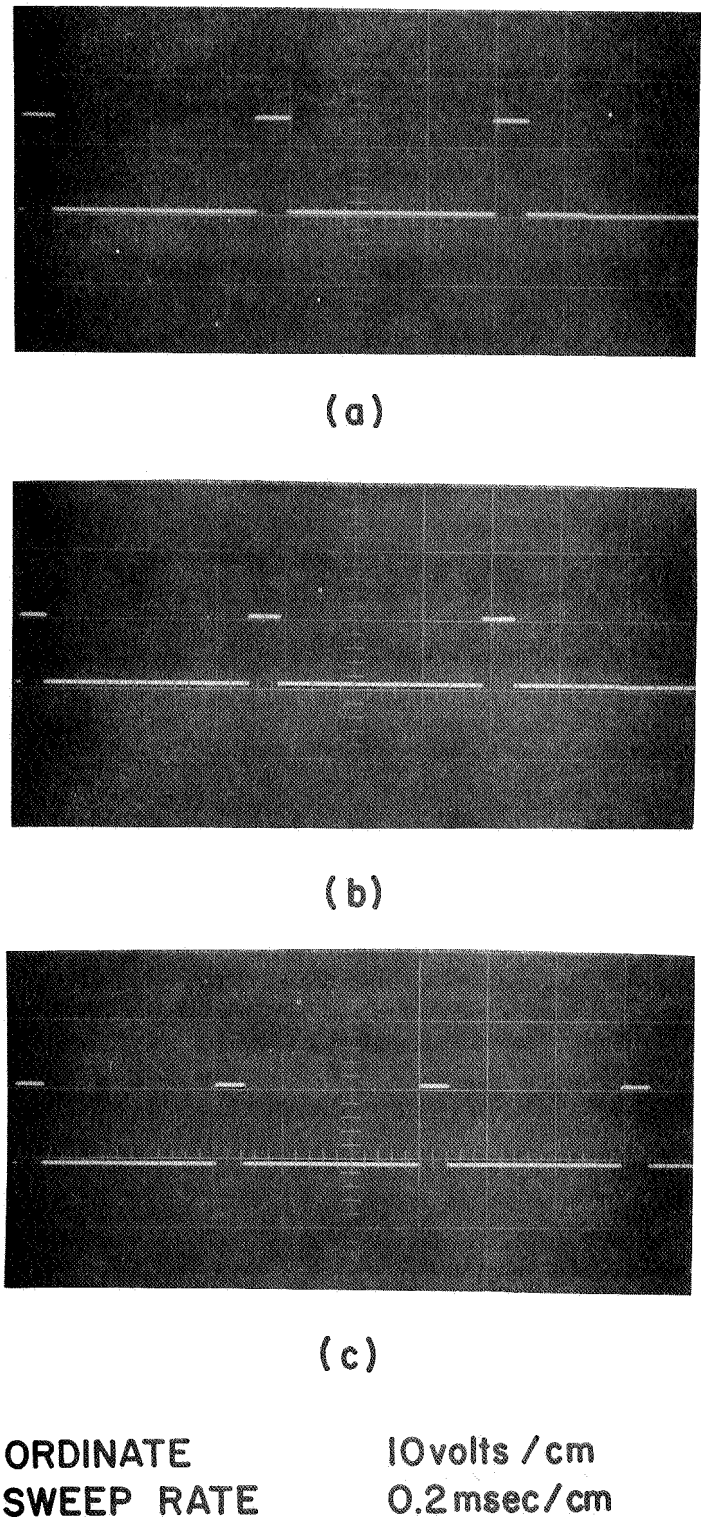

Figure 5.2 Typical output waveforms of the absorption signal simulator illustrating several different settings.

Since the selected echo is integrated, the shape of the simulated echo for test purposes is not particularly important, as long as the product of the pulse width and the pulse amplitude is a satisfactory representation of the anticipated signal. Moreover, since only one echo is studied at a given time, the amplitude of the echo selected by the gate generator (see Chapter 6) may be adjusted to the expected level. For example, if a comparison of the system response between the 1E-echo and the 2E-echo is required, the output of the absorption signal simulator for the LE-echo may be selected as 10 volts, whereas the output for the 2E-echo may be adjusted to 1 volt. Hence, a relative indication of the system response may be obtained in this manner.

6. THE SIGNAL ANALYSIS SUBSYSTEM

6.1 General Description

The purpose of the signal analysis subsystem is to measure automatieally the amplitude of the particular reflection to be studied and to provide a permanent record of the variation of this eeho. Assuming the system has been properly calibrated, the record is therefore a direct indieation of the variation in the degree of ionospheric absorption.

A block diagram of the signal analysis subsystem is shown in Figure 6.1. The signal from the pulse generator is used to trigger a gating eireuit which produces a gate pulse at a time determined by the particular eeho to be measured. This pulse is then gated with the return signal from the reeeiver and the resultant output of the eeho selector is the desired reflection, where all other echoes have been suppressed. The seleeted eeho is integrated, and the resultant de level is amplified to produce the necessary AGC voltage for the reeeiver. The output of the amplifier is also applied to a comparator eireuit and the difference between this voltage and a fixed referenee level is permanently recorded on a pen recorder.

Having briefly discussed the operation of the signal analysis subsystem, it is now possible to consider the individual circuits in the system and to analyze the performance of each circuit.

6.2 Gate Generators

As discussed in Chapter 1, the magneto-ionic theory shows that the amount of ionospherie absorption is inversely proportional to the square of the operating frequeney [Equation (1.15)]. For this reason, relatively low frequencies

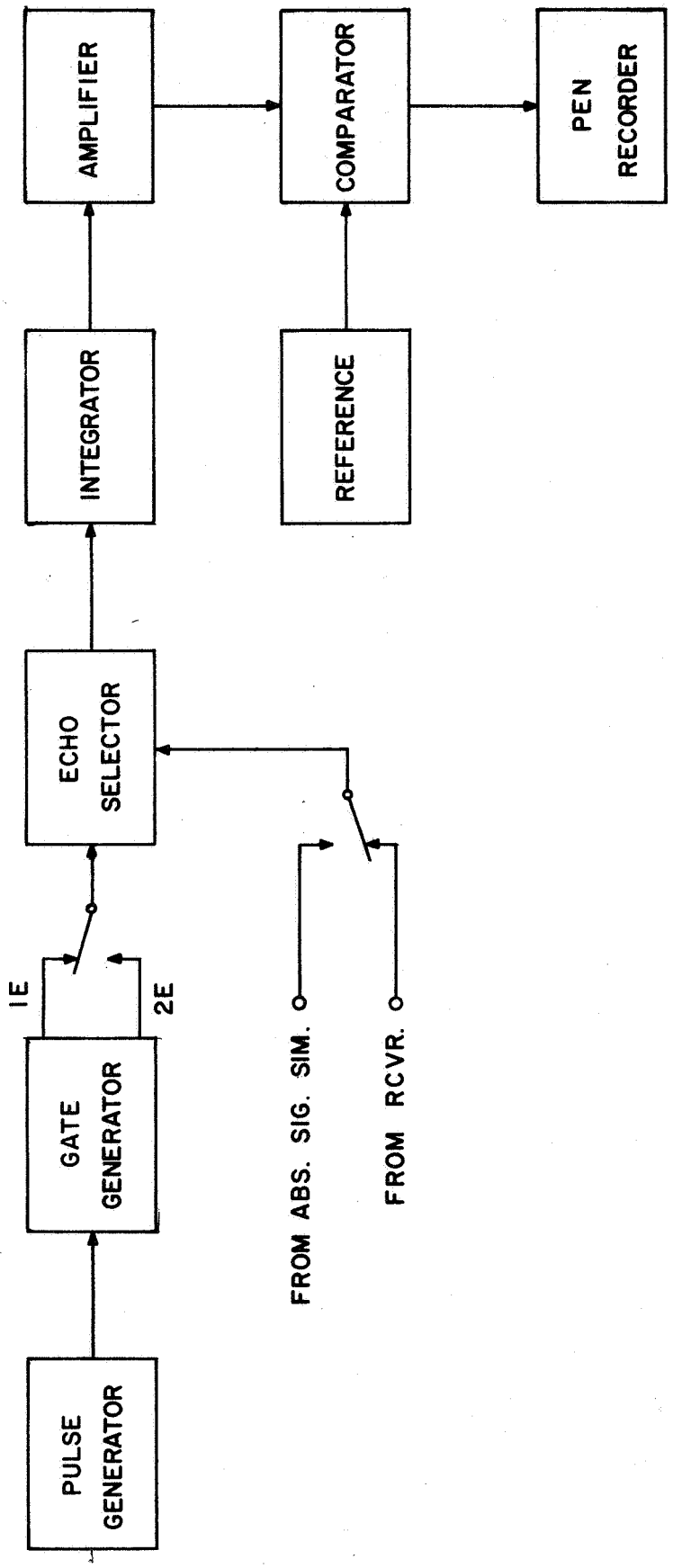

Figure 6.1 Block diagram of the signal analysis subsystem

(1.0 - 4.0 Mc/s) are generally selected for absorption measurements in order that the effect of absorption on the transmitted wave is significant enough to be measured accurately, Since the transmitted waves in this particular frequency range are reflected from the E-layer of the ionosphere, the gate generators of the signal analysis subsystem were specifically designed to select the 1E- and 2E-echoes from the return signal,

The schematic diagram of the 1E- and 2E-echo gate generators is shown in Figure 6.2. Assuming that the selector switch is in the LE-echo gate position, the output of the pulse generator is inverted and applied to a monostable multivibrator (MSMV). The output transistor of the MSMV remains in the "on" or unstable state for a time determined by the collector-base coupling time constant and by the base bias applied to the input transistor. The position of the pulse (i.e., the amount of time the output transistor remains in the unstable state) may be varied from approximately 0.3 to 1.0 msec by adjusting the base bias on the input transistor.

This signal is then applied to a Schmitt trigger, The output transistor of this circuit, which is initially "on", is turned "off" when the output transistor of the MSMV is turned "off". It then remains "off" for a time determined by the collector-base time constant. Hence, the width of the 1E-echo gate pulse may be varied from approximately 0.1 to 0.5 msec by adjusting the resistance of the collector-base time constant. The output of the Schmitt trigger is amplified and the resultant signal may be used to select the 1E-echo from the return signal.

The operation of the 2E-echo gate generator is identical to that of the 1E-echo gate generator. The time constants and biasing of the MSMV and Schmitt trigger circuits, however, are different. Hence, the position of the

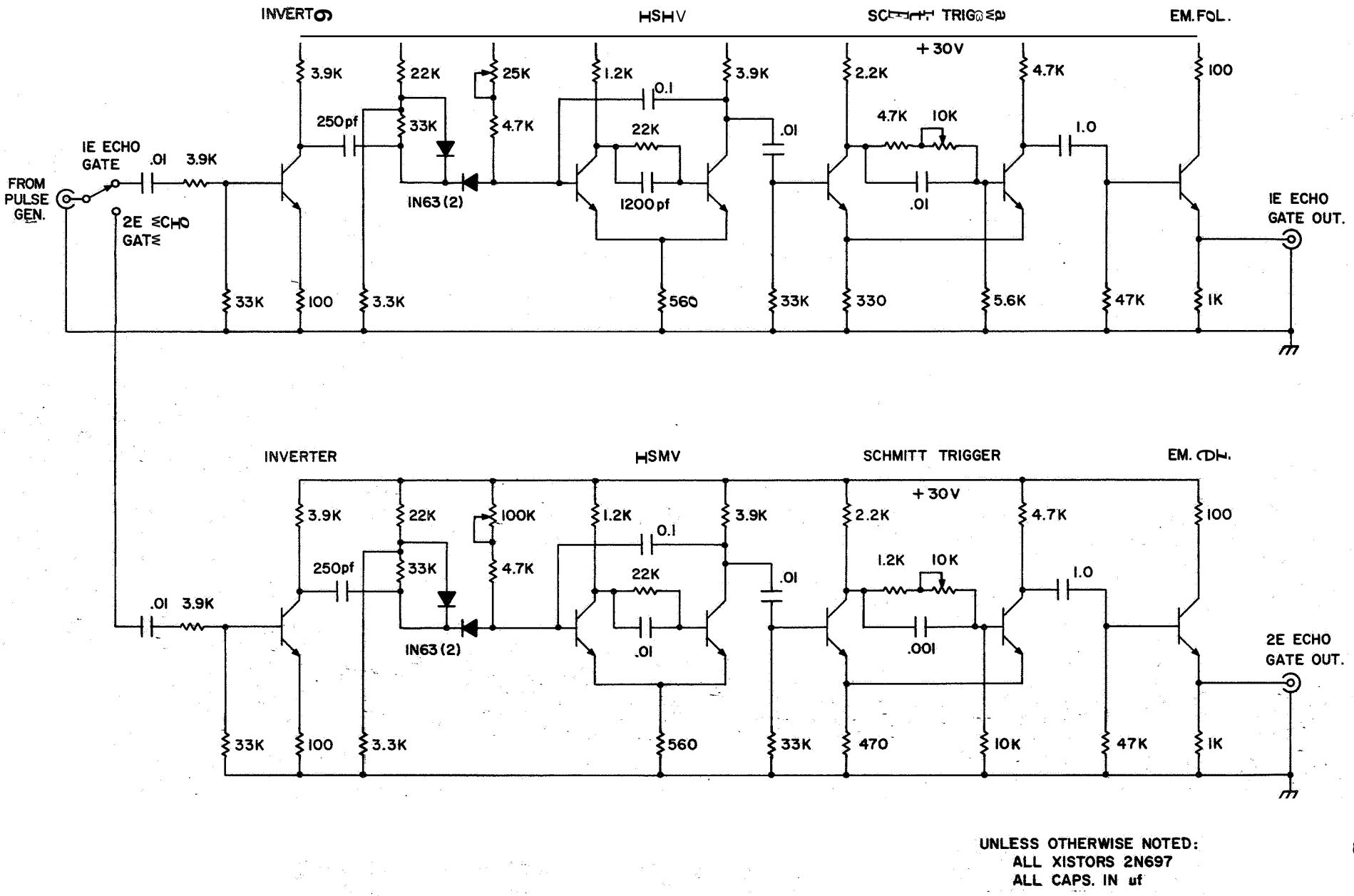

UNLESS OTHERWISE NOTED:
ALL XISTORS 2N697
ALL CAPS. IN uf

Figure 6.2 Schematic diagram of the 1E- and 2E-echo gate generators.

2E-echo gate pulse may be varied from approximately 1.0 to 2.0 msec by adjusting the base bias on the MSMV input transistor. The width of the 2E-echo gate pulse may be varied from approximately 0.1 to 0.5 msec by adjusting the resistance of the collector-base time constant of the Schmitt trigger.

It is possible to design one gate generator capable of covering the range of operation of the 1E-echo and 2E-echo gate generators. However, it is very useful to compare the absorption data obtained by using the 1E-echo to that obtained by measuring the 2E-echo. A typical sampling period for this type of study may consist of a ten minute measurement of the 1E-echo and a subsequent ten minute measurement of the 2E-echo. The availability of two separate generators facilitates this operation and eliminates continual adjustment of the gate pulse if only one gate generator is employed,

6.3 Echo Selector and Integrator

The schematic diagram of the echo selector and integrator circuits is shown in Figure 6.3. The purpose of this unit is to select the desired sky wave reflection from the return signal, and to provide a dc output voltage proportional to the peak amplitude of the selected pulse,

The eeho selector is a conventional two input "and" gate directly coupled to an emitter follower. The output of the gate generator is applied to one input and the return signal from the receiver is fed into the other input. Only that portion of the return signal which falls within the gating period is passed by the gate. The gate pulse is adjusted to include the echo to be studied and all other echoes and associated noise are suppressed,

Various waveforms illustrating the operation of the eeho selector are shown in Figure 6.4. Figure 6.4a shows the output of the absorption signal

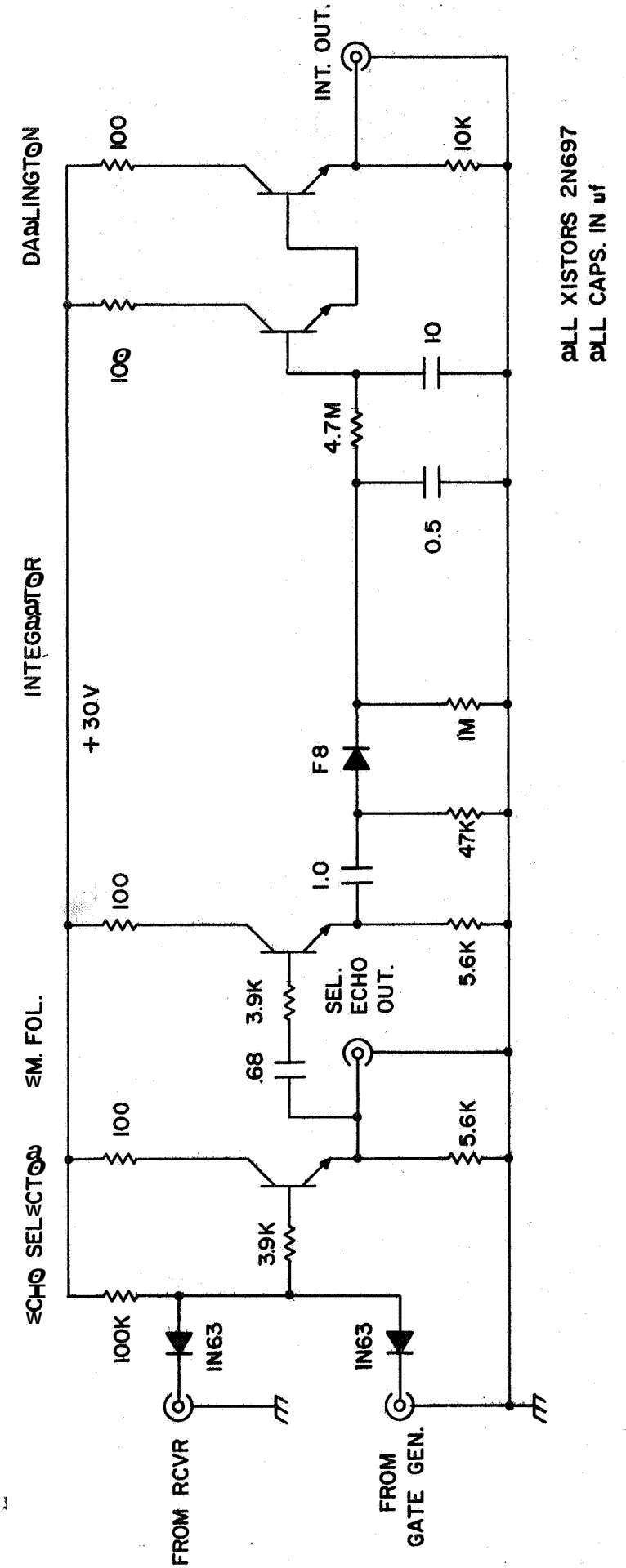

Figure 6 3 Schematic diagram of the echo selector and integrator

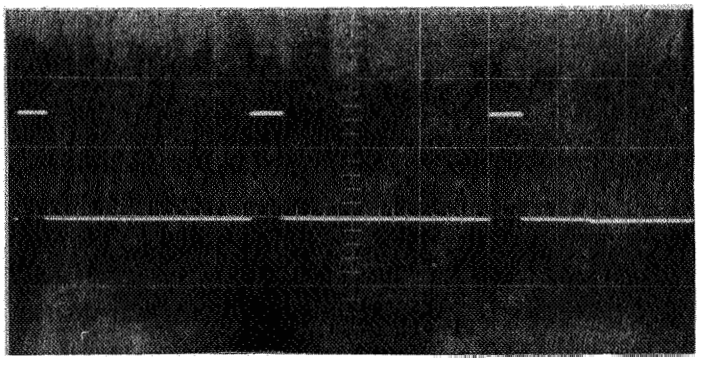

(a)

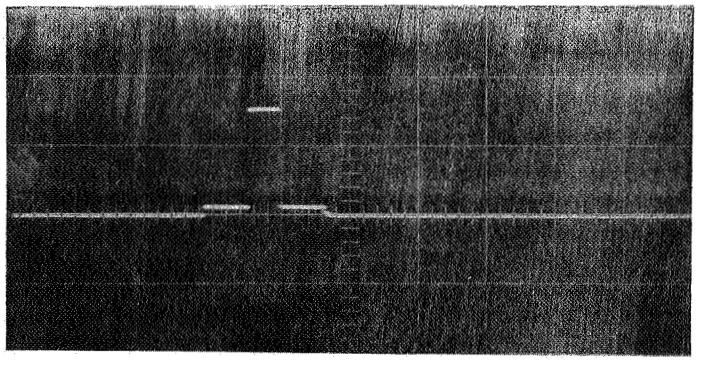

(b)

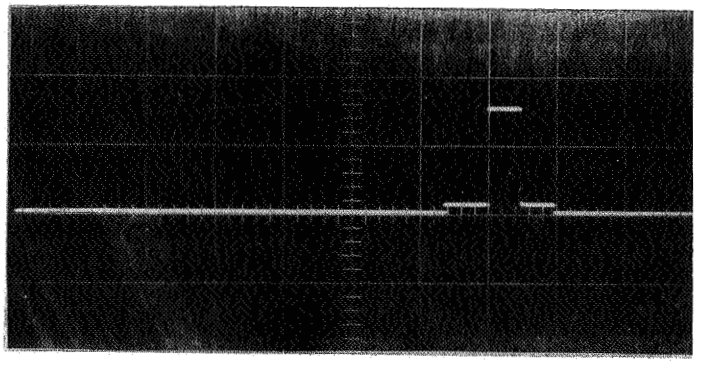

(c)

ORDINATE 10 volts / cm
SWEEP RATE 0.2 msec / cm

Figure 6.4 Various waveforms illustrating the operation of the echo selector.

simulator consisting of the ground pulse, the 1E-echo (105 km), and the 2E-echo (210 km). Figure 6.4b depicts the case where the 1E-echo has been selected from the simulated signal; the width of the 1E-echo gate pulse being 0.35 msec. The case in which the 2E-echo has been gated from the simulated signal is shown in Figure 6.4c, where the width of the 2E-echo gate pulse is also 0.35 msec.

There is a constant dc level or "pedestal" of approximately 0.7 volts associated with the generation of the gate pulse as shown in Figure 6.4. This allows visual positioning of the gating period, Since this level is integrated along with the selected echo pulse, its effect must be eliminated by properly calibrating the system taking this level into account.

The output of the echo selector is coupled to a peak detector by means of an emitter follower. The 0.5 μf capacitor can be fully charged in the duration of a few pulses and can discharge fast enough, with its time constant of 0.5 sec, to follow accurately the fading of the pulse signal; assuming that the average fading period is of the order of 5 to 10 sec.

The output of the peak detector is connected to an integrator circuit with a time constant of 47 sec, so that the output voltage is effectively a "running mean" of the signal amplitude over this time. As mentioned in Chapter 4, the capacitor of the integrator circuit must have low leakage. For this reason, five 2 μf mylar capacitors were carefully selected and connected in parallel to obtain the required capacitance.

To eliminate any change in the time constant of the integrator circuit by external loading, the output of the integrator is connected to a Darlington circuit, which has a very high input'impedance approximately equal to the product of the common-emitter forward current gain (h_{fe}) squared and the emitter resistance

of the output transistor. The transistors selected for this stage have a minimum h_{fe} of 70, so that the effective input impedance of this circuit is approximately 50 megohms. Since this value is much greater than the 4.7 megohm resistor of the integrator time constant, the effect of loading on the integrator circuit is essentially eliminated.

6.4 Amplifier and Comparator

The slowly-varying dc output of the Darlington circuit is directly coupled to a two-stage dc amplifier to provide the necessary AGC voltage for the receiver, The AGC voltage is also applied to a comparator circuit and the difference between this voltage and a fixed reference level is permanently recorded.

A schematic diagram of the dc amplifier and comparator circuits is shown in Figure 6.5. The first stage of the dc amplifier is a differential amplifier consisting of transistors Q_1, Q_2 and Q_5. Under the assumptions that the base-emitter voltage drop of the transistors is negligible and that the common-base forward current gain (h_{fb}) is unity, it can be shown that the open-loop gain of the first stage is approximately equal to the ratio of the collector resistance of Q_1 and the sum of the emitter resistances of Q_1 and Q_2. A constant current source (Q_5) is used to produce the required emitter current and to stabilize the operation of the differential amplifier.

The output of the first stage, which is proportional to the difference between the voltages applied to the bases of Q_1 and Q_2 is further amplified by a second stage consisting of transistors Q_3 and Q_4. The total open-loop gain, G_o, of the amplifier, therefore, is the product of the individual gains of the first and second stages. With the values indicated in Figure 6.5, the open-loop gain of the dc amplifier is approximately 60,

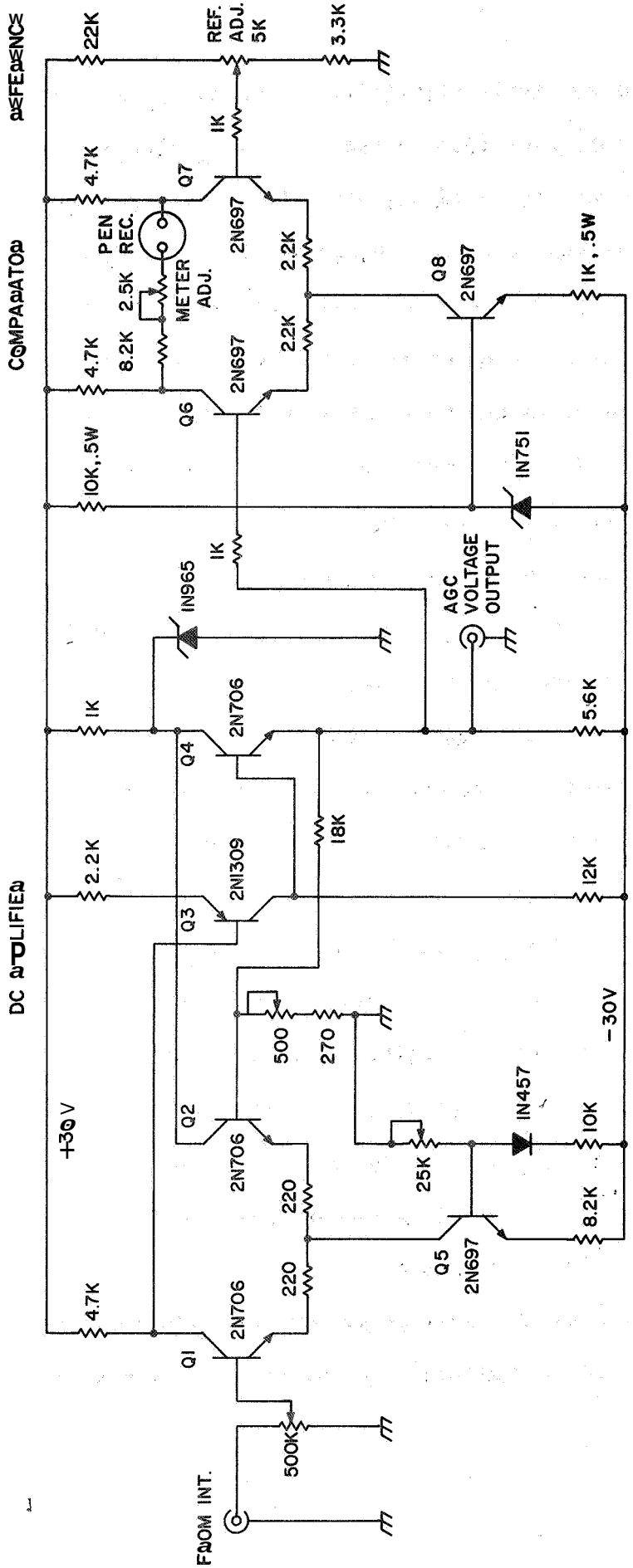

Figure 6.5 Schematic diagram of the dc amplifier and comparator.

For increased circuit stability, a feedback path is employed from the emitter of the output transistor (Q_4) to the base of Q_2 of the differential amplifier. The feedback network is an adjustable voltage divider; the amount of the output signal applied to the base of Q_2 being equal to the ratio of the resistance from the base of Q_2 to ground and the total resistance from the emitter of Q_4 to ground.

If the amount of feedback is designated by f, the closed-loop gain, G, of the system may be expressed as $G_o/(1 + fG_o)$. By changing the value of f, the closed-loop gain of the dc amplifier in Figure 6.5 may be varied from 6 to 18, This gain is sufficient to provide the necessary AGC voltage for the receiver over the expected range of input amplitudes.

The output of the dc amplifier is coupled to the base of Q_6 of a comparator circuit, which is essentially a differential amplifier. A fixed reference voltage is applied to the base of Q_7, The difference in the collector voltages of these two transistors is then measured by a dc micro-ammeter (0 - 500 pa) of an Amprobe pen recorder. A constant current source (Q_8) is used to provide additional circuit stability.

For normal operations, the reference voltage is selected at 5.4 volts, which is the minimum AGC voltage that can be applied to the receiver (see Figure 3.5). The circuit is calibrated by applying the fixed reference voltage simultaneously to the bases of Q_6 and Q_7 and observing the current reading. If the circuit is balanced, the collector voltages are equal and, hence, the meter is zeroed. It was necessary to select matched transistors for Q_6 and Q_7 in order to obtain a balanced circuit,.

Since the maximum AGC voltage for the receiver was selected as 11 volts, it is also necessary to calibrate the meter for a full-scale reading of 500 µa

with the application of this voltage. This was accomplished by simultaneously applying a fixed value of 11 volts to the base of Q_6 and the reference voltage of 5.4 volts to the base of Q_7. The resistance between the collectors is then adjusted until a full-scale deflection of the meter is obtained. Hence, the input voltage (i.e., the receiver AGC voltage) is linearly proportional to the current measured in microamperes. The meter reading is permanently recorded on a strip chart, thus giving an immediate indication of the amount of ionospheric absorption,

In order to facilitate the calculation of electron density profiles from the absorption data (see Chapter 8), an alternate method of recording the receiver AGC voltage (and, therefore, the amount of ionospheric absorption) will be employed, The output of the dc amplifier will be measured by a digital voltmeter and recorded by a Tally punched-tape recorder (see Figure 4.1). The data will then be in a form amenable to further calculations on a computer,

6.5 Mathematical Analysis of the Signal Analysis Subsystem

It is difficult to analyze the operation of the automatic recording system, since the AGC characteristic curve of the receiver cannot accurately be expressed mathematically. However, if a linear approximation of the curve is assumed, the following analysis may be made,

The receiver AGC characteristic curve may be linearly expressed over a limited range as

$$\log_{10} \alpha = A - \frac{A}{V_b} V_a \qquad (6.1)$$

where α is the gain of the receiver, V_a is the receiver AGC voltage, V_b is a constant equal to V_a when $\alpha = 1$, and A is the value of $\log_{10} \alpha$ when $V_a = 0$.

Referring to Figure 6.1, the output of the receiver is αI, where I is the amplitude of the particular reflection to be measured. The input to the integrator is $K_1 \alpha I$, where K_1 is the circuit gain constant of the echo selector. If the gain constant of the integrator is designated as K_2 and the gain of the de amplifier as K_3, the resultant AGC voltage, V_a, for the receiver may be expressed as $K_1 K_2 K_3 \alpha I$.

The output of the comparator circuit, V_c, may then be written as

$$V_c = K_4 (V_a - V_o) \tag{6.2}$$

where K_4 is the gain constant of the cornparator circuit and V_o is the fixed reference voltage, This equation may be expressed as

$$V_c = K_5 \alpha I - K_4 V_o \tag{6.3}$$

or,

$$\alpha I = \frac{V_c + K_4 V_o}{K_5} \tag{6.4}$$

where K_5 is the resultant gain constant of K_1, K_2, K_3, and K_4. Rewriting equation (6.4) in logarithmic form gives

$$\log_{10} I = \log_{10} \frac{V_c + K_4 V_o}{K_5} - \log_{10} \alpha \tag{6.5}$$

and substituting equation (6.1) into this expression yields

$$\log_{10} I = \log_{10} \frac{V_c + K_4 V_o}{K_5} + \frac{A}{V_b} V_a - A \tag{6.6}$$

As shown in Chapter 2, the amount of ionospheric absorption, L, is proportional to the logarithm of the amplitude of the reflection to be studied, assuming, of course, that the transmitter output power is constant. It is evident from equation (6.6) that the variation of ionospheric absorption is linearly proportional to

$$\log_{10} \frac{V_c + K_4 V_o}{K_5} + \frac{A}{V_b} V_a \qquad (6.7)$$

where the only variable is V_a, since V_C is determined by the value of V_a (Equation 6.2).

Examination of equation (6.7) shows that the variation of absorption is almost directly proportional to V_a, since the quantity $\log_{10} [(V_c + K_4 V_o)/K_5]$ varies much more slowly than the quantity AV_a/V_b. This is especially true when the value of V_a is small.

Therefore, if a voltage directly proportional to the receiver AGC voltage V_a is recorded (e.g., V_c), it will vary almost linearly according to the variation in the amount of ionospheric absorption. The absorption level, L, may then be read directly from the pen recorder, providing the scale has been suitably calibrated,

7. THE ECHO-HEIGHT RECORDING SUBSYSTEM

7.1 Purpose of the System

The purpose of the echo-height recording subsystem is to measure automatically the apparent height at which a radio wave is reflected from the ionosphere. This data is useful in that it gives a relative indication of the variation in the reflection layer being studied.

Moreover, as discussed in Chapter 2, the amount of ionospheric absorption, L, is dependent on the apparent height of reflection. Equation (2.10) may be expressed as

$$L = 20 \log G - 20 \log I_1 - 20 \log h' \qquad (7.1)$$

where I_1 is the first-order echo, G is a calibration constant, and h' is the apparent height of reflection. Hence, for precise calibration of the automatic recording system, it is useful to have some indication of how the value of h' is varying. Moreover, if the visual measurement technique discussed in Chapter 3 is employed, it is necessary to determine h' before the final calculation of the absorption level, L, may be made.

7.2 General Description

A block diagram of the echo-height recording subsystem is shown in Figure 7.1. The output of the pulse generator is used to set a bistable multivibrator (BSMV) circuit. This pulse is then gated with a crystal-controlled square wave generator and the gate remains open until the BSMV is reset by the particular reflection passed by the echo selector. The resultant output of the gate, therefore, is the number of cycles of the square wave

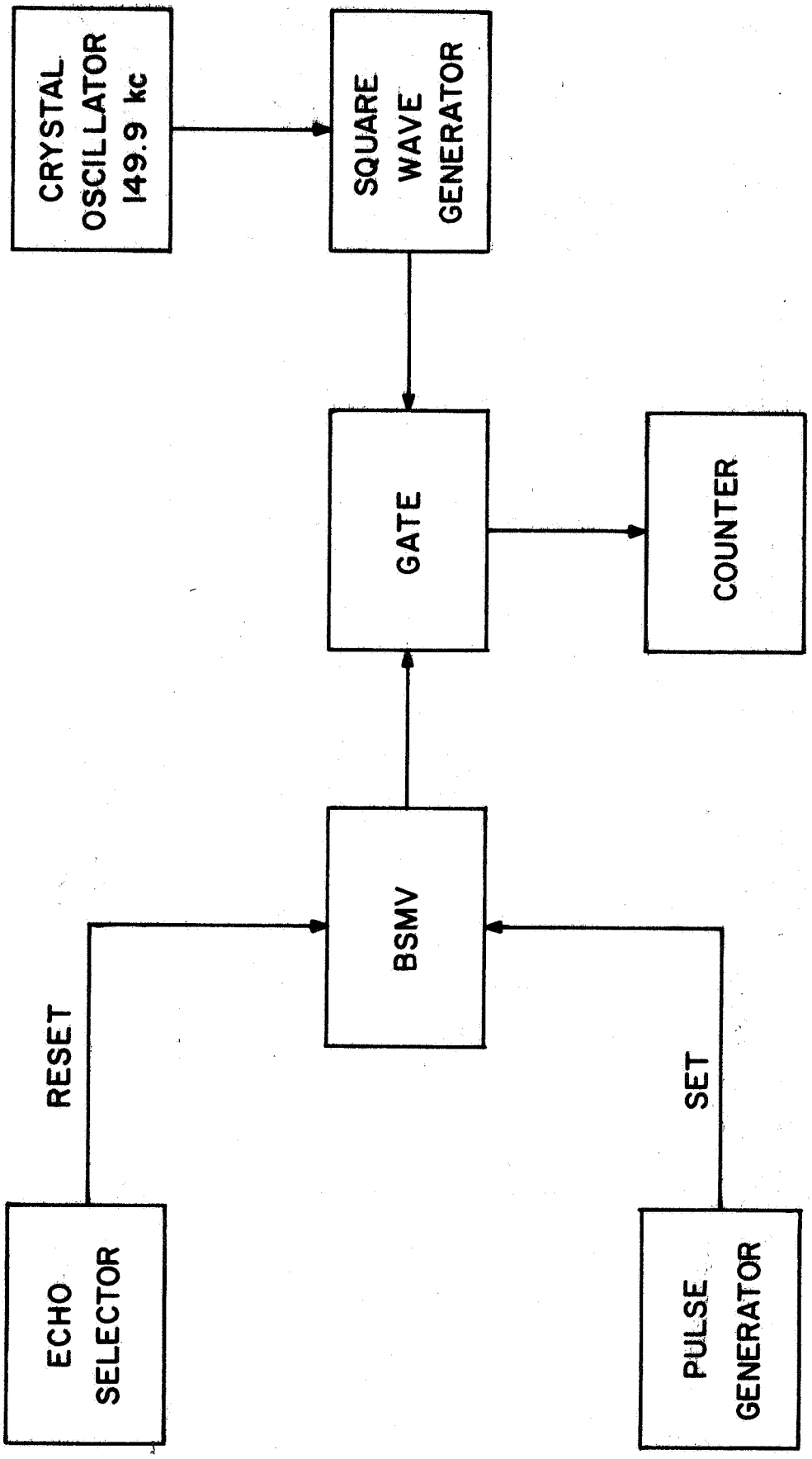

Figure 7.1 Block diagram of the echo-height recording subsystem.

generator frequency which fall within the gating period. The number of cycles is recorded on an electronic counter, thus giving a relative indication of the apparent height at which the particular reflection of the radio wave occurs.

A schematic diagram of the echo-height recording subsystem is shown in Figure 7.2, The gate pulse is produced by a set-reset bistable multivibrator circuit. The output transistor of the **BSMV,** which is initially "on", is turned "off" (set) by the output of the pulse generator. It then remains in this state until it is turned "on" (reset) by the output of the echo selector. The width of the gate pulse, therefore, is equal to the elapsed time between the transmission of the pulse and the subsequent reception of the particular echo to be studied,

The square wave generator consists essentially of a crystal-controlled sine-wave oscillator and a Schmitt trigger. The oscillator is a conventional tuned-tank circuit in which positive feedback is employed through a series crystal, The sine-wave output of the oscillator is then converted to a pulse waveform by use of the Schmitt trigger; the width of the pulse being determined by the collector-base time constant. The width of the pulse is not particularly important providing that it is sufficient to be recorded by the counter,

As mentioned in Chapter 4, the apparent height at which a radio wave is reflected from the ionosphere is equal to one-half the product of the speed of light and the time required for the wave to travel to the ionosphere and back. It can be shown that one cycle of 149.900 kc/s corresponds to an apparent distance of 1 km, assuming the speed of light as 2.998×10^5 km/sec. Hence, this particular operating frequency was chosen for the oscillator circuit. The number of cycles recorded on the counter, therefore, is *a* direct indication of the apparent reflection height of the radio wave in kilometers.

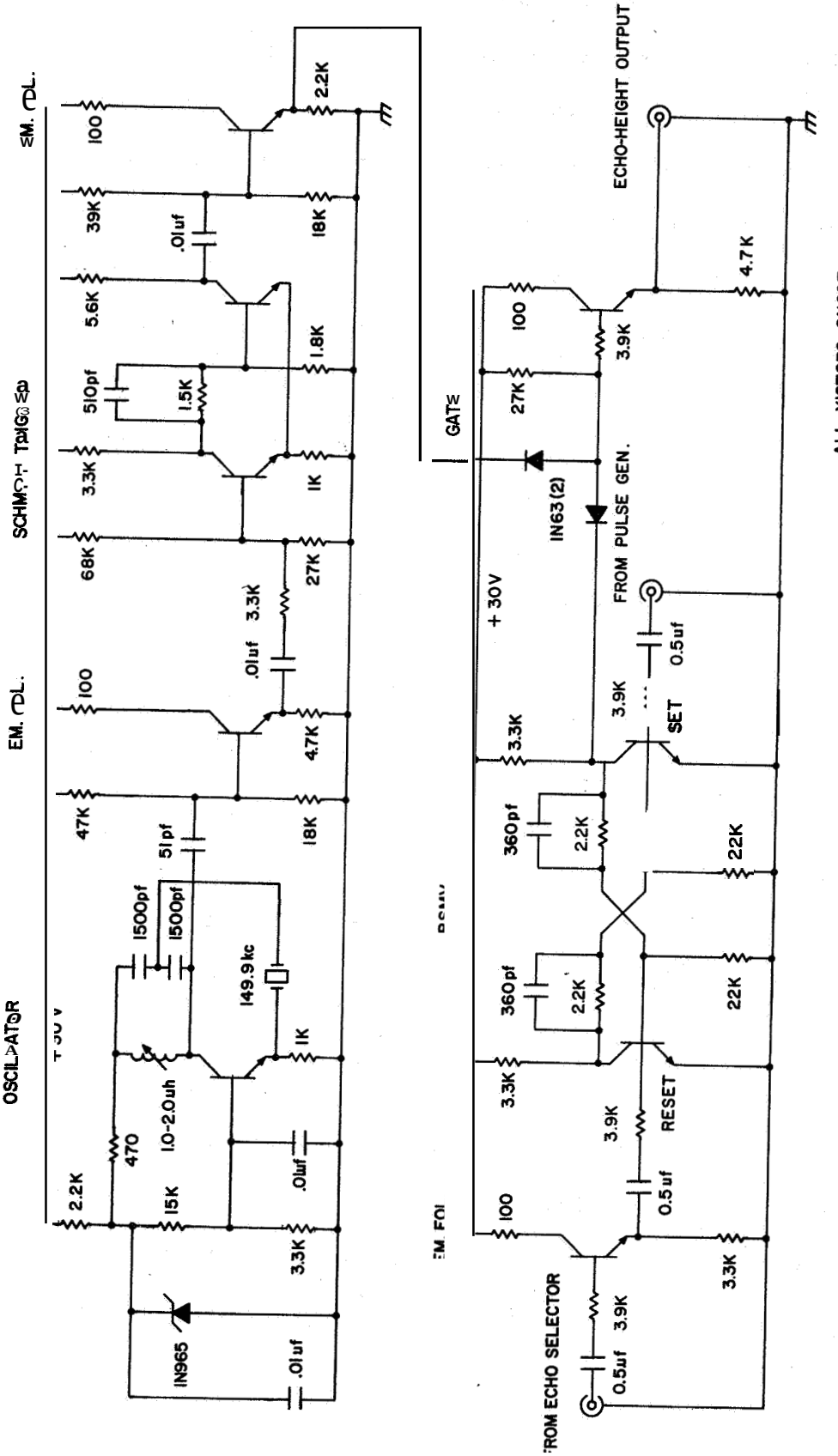

Figure 7.2 Schematic diagram of the echo-height recording subsystem.

Typical waveforms of the echo-height recording subsystem are shown in Figure 7.3. Figure 7.3a shows the output of the absorption signal simulator consisting of the ground pulse, the 1E-echo (105 km), and the 2E-echo (210 km). The case in which the apparent reflection height of the 1E-echo is measured is shown in Figure 7.3b. The number of cycles of the oscillator frequency recorded by the counter would be 105 cycles for this case. Figure 7.3c depicts the case in which the apparent height of reflection of the 2E-echo is measured. The counter would, therefore, record 210 cycles, corresponding to an apparent height of reflection of 210 kilometers, Any change in the apparent reflection height of the selected echo will cause a corresponding change in the width of the gate pulse; hence, as the apparent reflection height varies, the number of cycles recorded by the counter will vary accordingly.

7.3 Practical Design Considerations

Since the oscillator circuit of the echo-height recording subsystem operates continuously, the gate pulse may start and end at any time during a particular cycle of the operating frequency. Hence, the number of cycles recorded by the counter is accurate to ± 1 cycle, *or* $\pm$ 1 km of height. This accuracy is sufficient for all proposed applications of the system.

It is evident from Figure 7.3 that the echo-height recording subsystem measures the time delay between the initial occurrence of the ground pulse and the time at which the selected echo begins to occur. In practice, the return signals are not rectangular pulses as shown in Figure 7.3, but are Gaussian-shaped due to the effect of the tuned circuits in the receiver. This method of measuring the time delay, however, is still valid and no appreciable error

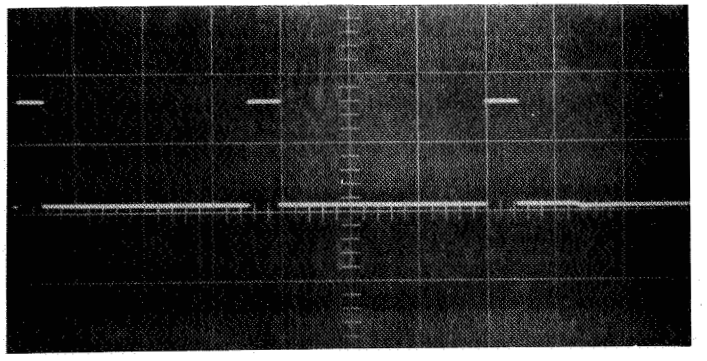

(a)

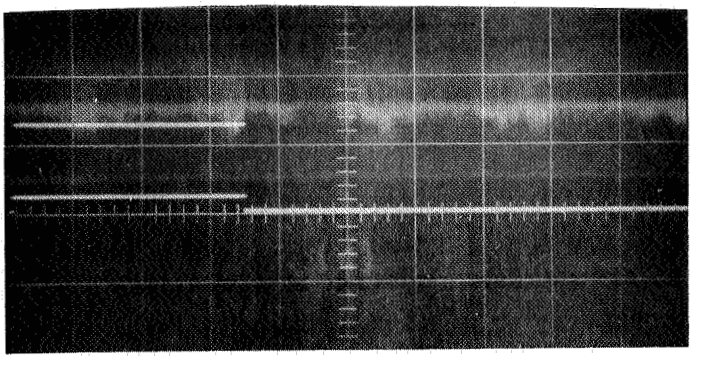

(b)

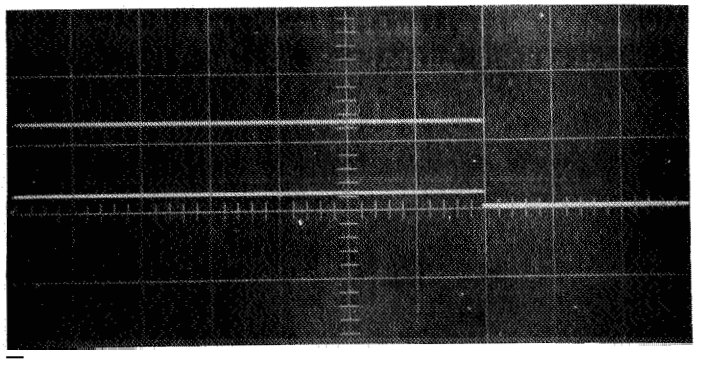

(c)

ORDINATE 10 volts / cm
SWEEP RATE 0.2 msec / cm

Figure **7.3** Various waveforms illustrating the operation of the echo–height recording subsystem.

is introduced into the measurement of the apparent reflection height by this technique.

An alternate method of determining the time delay between the ground pulse and the selected reflection is to measure the difference between the times of occurrence of the peak amplitudes of the two pulses. However, in cases where there is severe "splitting" of the selected echo, this method is not valid. When "splitting" is present, two or more peaks will usually occur and the system will only measure the time of occurrence of the first peak. This is not the same time of occurrence of the peak which would occur if there were no "splitting". This problem is not encountered in the technique presently being employed and no additional precautions need be taken in this regard.

8. SUMMARY AND CONCLUSIONS

Typical absorption records of the automatic recording system are shown in Figures 8.1 and 8.2. Figure 8.1a shows the scaling of the pen recorder and a calibration of the system using the 1E- and 2E-echoes. The recorder scaling curve is obtained by applying various values of the receiver AGC voltage to the comparator circuit; each value of the applied voltage corresponding to a 5 db increment of receiver attenuation (Figure 3.5). The recorded meter reading is thus a direct indication of the gain of the receiver for a given value of the AGC voltage.

Calibration of the system is accomplished by alternately measuring the amount of absorption of the LE- and 2E-echoes. From equation (2.10), the calibration constant of the system, 20 Log G, may be expressed as

$$20 \text{ Log } G = 20 \log I_1 + 20 \log h' + L \qquad (8.1)$$

where I_1 is the amplitude of the LE-echo, h' is the apparent reflection height, and L is the amount of ionospheric absorption equal to $-20 \log \rho$.

Moreover, the amount of absorption determined by measurement of the 2E-echo [Equation (2.11)] may be written as

$$2L = 20 \log G + 20 \log p_g - 20 \log I_2 - 20 \log (2h') \qquad (8.2)$$

where I_2 is the amplitude of the 2E-echo and p_g is the apparent reflection coefficient of the ground, Assuming that p_g is unity (i.e., the ground is a perfect reflector), substitution of equation (8.1) into this expression yields

$$L = 20 \log I_1 - 20 \log I_2 - 20 \log (2h'/h'). \qquad (8.3)$$

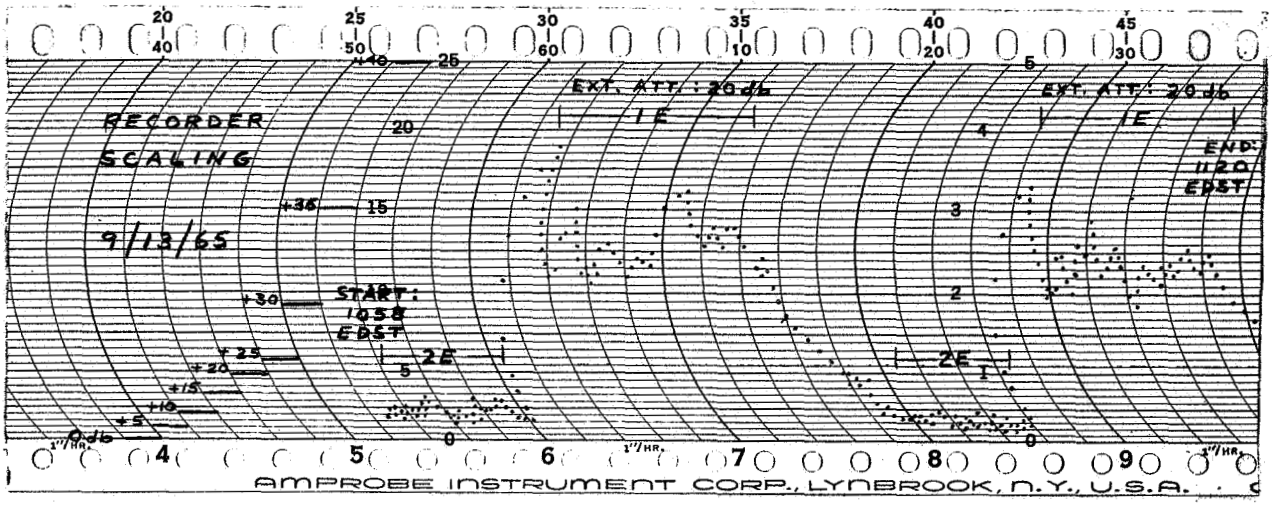

(a)

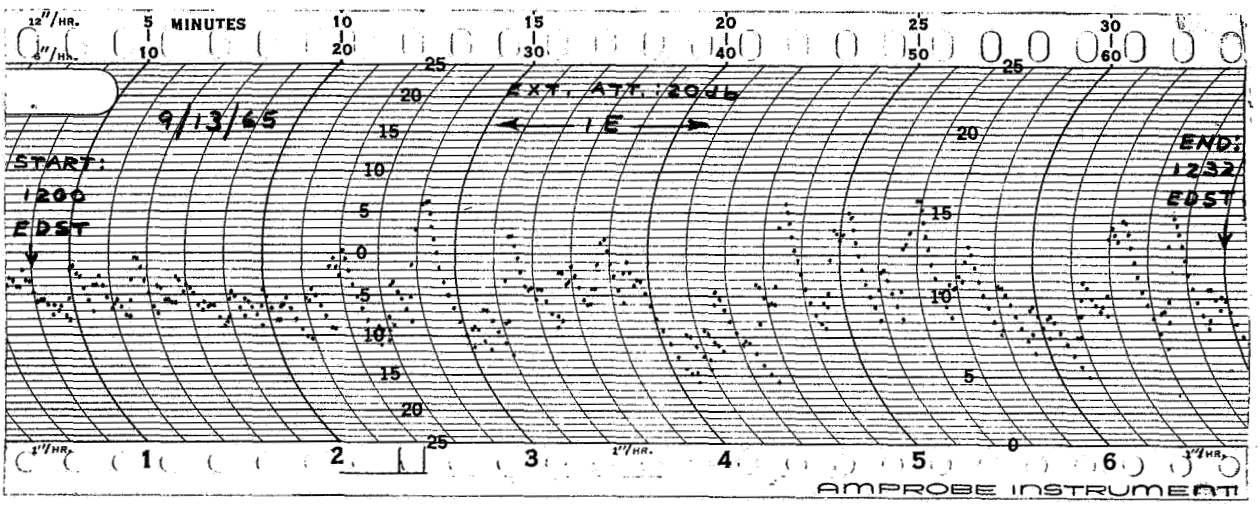

(b)

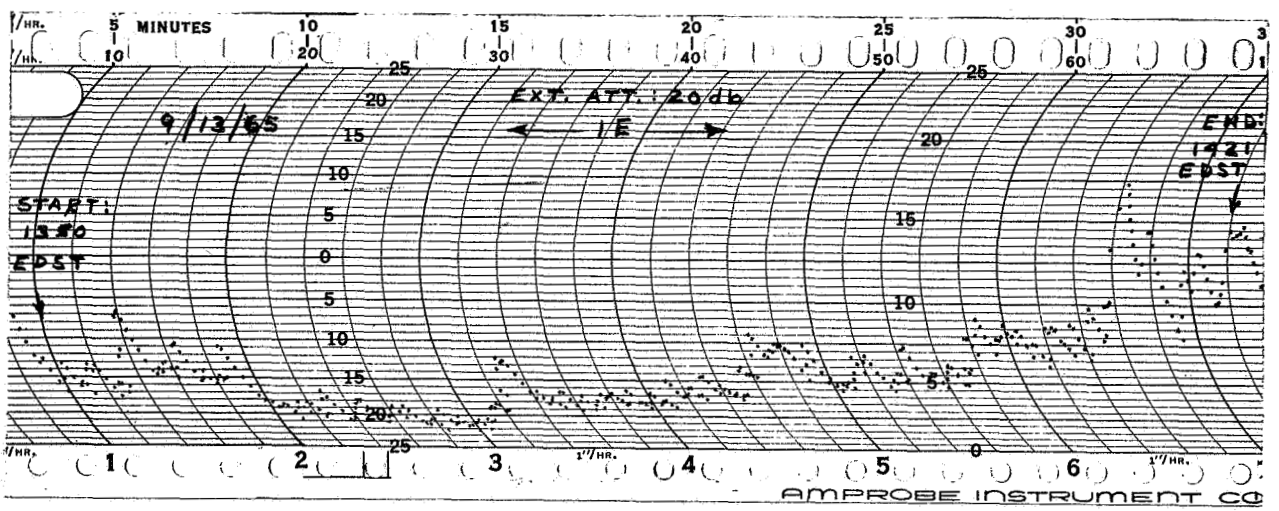

(c)

Figure 8.1 Typical records of the automatic recording system illustrating the variation in absorption of the 1E-echo.

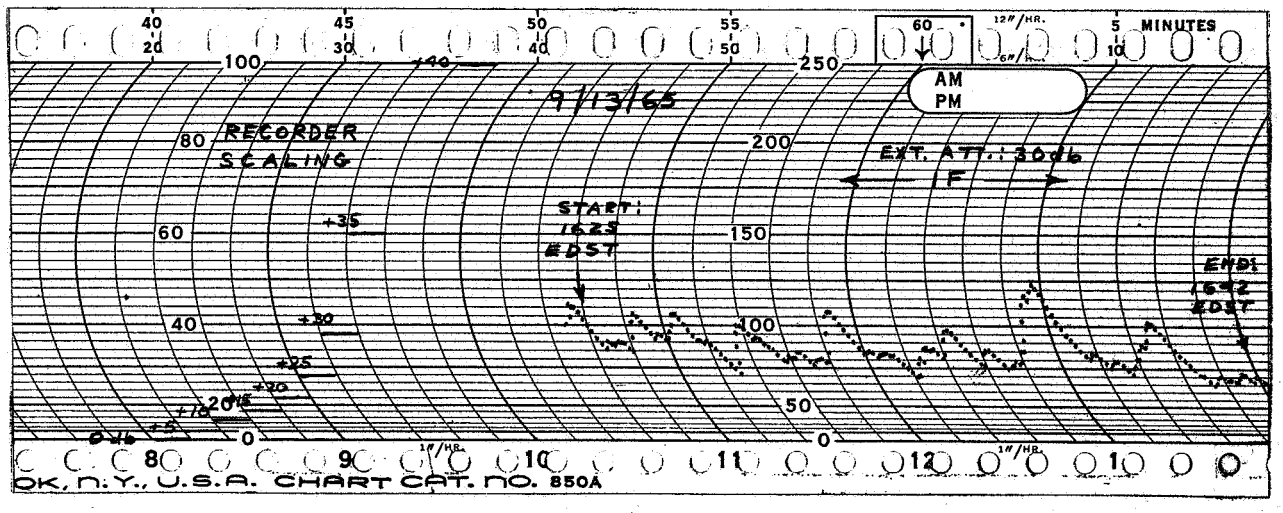

(a)

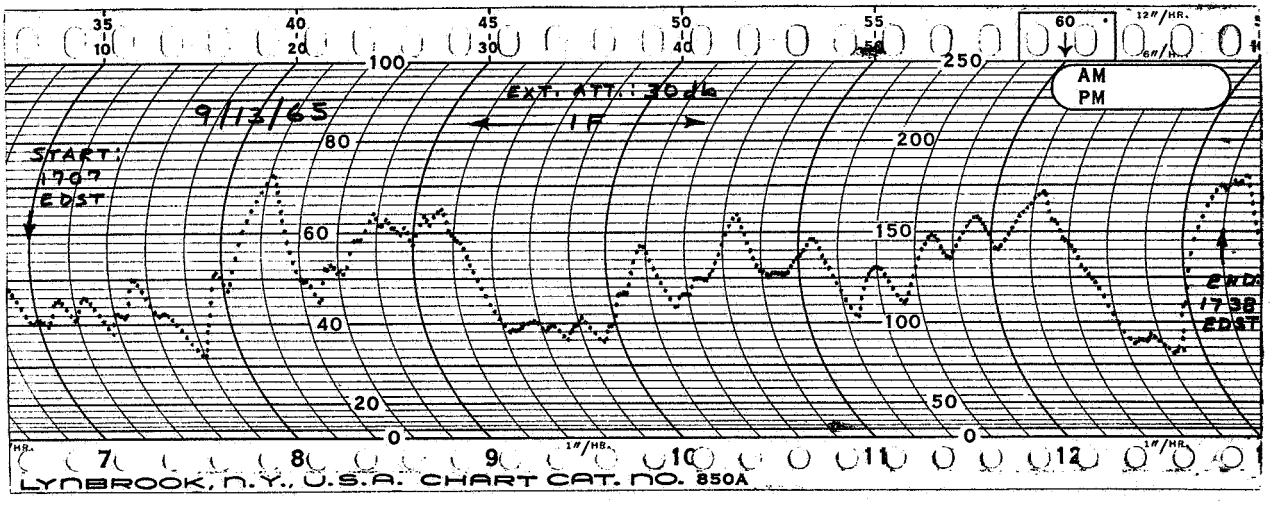

(b)

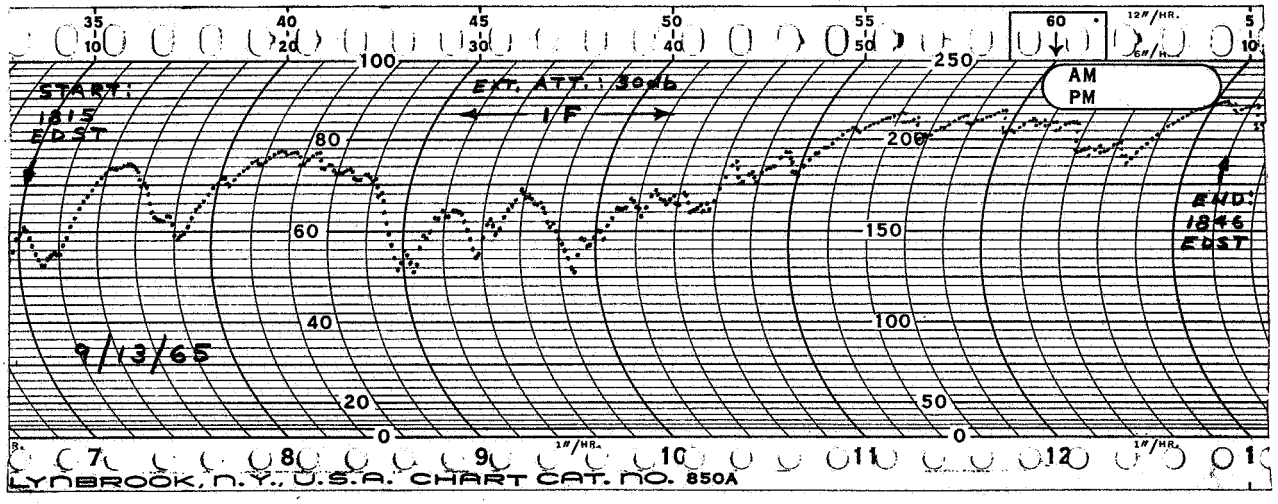

(c)

Figure 8.2 Typical records of the automatic recording system illustrating the variation in absorption of the 1F-echo.

Hence, by alternately measuring the values of 20 log I_1 and 20 log I_2, the amount of ionospheric absorption, L, for a given sampling period may be determined. This value may then be substituted into equation (8.1) to obtain the calibration constant of the system, 20 log G.

In general, the measurements of 20 log I_1 and 20 log I_2 are usually made at night when the absorption is relatively small. However, at the particular time that measurements were being made, the transmitted signal penetrated the E-layer during the nighttime hours. Hence, it was necessary to calibrate the system during the day when E-layer reflections were present. Little error was introduced into the system calibration since the amplitudes of the observed echoes were sufficiently large to be measured accurately.

Referring to Figure 8.1a, the mean value of 20 log I_1 for the sampling period is 52 db, including the 20 db external attenuation, and the mean value of 20 log I_2 is 8 db. Since the value of 20 log (2h'/h') is 6 db, the amount of ionospheric absorption, L, for the sampling period is 38 db. The apparent height of reflection of the 1E-echo was determined to be 115 km by use of the echo-height recording subsystem; hence, the value of 20 log h' is approximately 41 db. From equation (8.1), the calibration constant of the system, 20 log G, is therefore 131 db. Assuming that there is no significant change in the apparent reflection height during subsequent measurements, the amount of absorption at any given time may then be obtained by simply subtracting the recorded value of 20 log I_1 from 90 db (i.e., 20 log G - 20 log h').

For example, Figure 8.1b shows the variation of absorption from 1200 EDST to 1232 EDST. The value of 20 log I_1 remains essentially constant at approximately 50 db. Hence, the amount of ionospheric absorption is approximately

40 db during this period. Figure 8.1c illustrates the ease in which the absorption reaches its maximum level (i.e., the amplitude of the received reflection is a minimum). The amount of absorption increases from a value of approximately 52 db at 1350 **EDST** to a maximum value of 60 db at 1400 **EDST.** It then gradually decreases to 45 db at 1420 **EDST.**

A typical record of the absorption of the 1F-echo during sunset is shown in Figure 8.2. The recorded value of the P-echo amplitude is approximately 57 db at 1625 **EDST** and gradually increases to a value of 69 db at 1846 **EDST.** This corresponds to a decrease of 12 db in ionospheric absorption over this time. This record clearly demonstrates the effect of the sun's radiation on the amplitude of radio waves reflected from the ionosphere.

As a result of the records obtained, proposed modifications of the automatic recording system to optimize its performance include the following:

(i) Increasing the dynamic range of the AGC system from 40 db to approximately 70 db to eliminate the necessity of changing scales by use of an external attenuator,

(ii) Modifying the AGC circuit to linearize the receiver AGC characteristic, thus permitting a more linear variation of absorption with recorder deflection.

The ultimate objectives of absorption studies are to interpret the absorption data in terms of the ionization density and collision frequency as functions of height in the absorbing region and to determine how these functions vary with such factors as time of day, geographical location, and solar activity. Future investigations of absorption phenomena will include a comparison of the results obtained from the sounding rocket program of the Aeronomy Laboratory and that obtained by use of the automatic recording system.

Moreover, it is anticipated that the existing sounding system will be modified to transmit and receive two or more different frequencies, A comparison of the absorption data obtained on the different frequencies may then be used to calculate an electron density profile of the ionosphere over a limited height range. The punched-tape recording system described in Chapter 4 will be employed in order that the obtained data will be in a form amenable to calculation of the electron density profile on a computer. In addition to recording absorption data, the punched-tape system will be commutated to record apparent reflection height data obtained by the echo-height recording subsystem,

Shapley and Beynon (1965) have recently proposed a new application for absorption measurements. Their work has shown that there is a definite correlation between the winter anomaly in ionospheric absorption and the temperature in the upper stratosphere at middle latitudes. Specifically, they established that the temperature at the 10 mB level (approximately 30 km) was highly dependent on the change in the amount of ionospheric absorption in the D- and lower E-regions; the greater the absorption, the higher the temperature at this level. Future investigation of this phenomenon might consist in a program of selected rocket firings at times when the amount of ionospheric absorption is abnormally high. Temperature and pressure data could be obtained by the rocket and compared with simultaneous measurements of absorption obtained by the automatic recording system, thus giving a new insight into the mechanisms producing this effect.

It is evident from the preceding discussion that the measurement of absorption is a powerful technique in the study of ionospheric phenomena. The automatic recording system will permit a more extensive absorption measurement

program with a greater economy of effort than the visual measurement method presently being used by the Aeronomy Laboratory.

BIBLIOGRAPHY

Appleton, E. V. and Piggott, W. R., "Ionospheric Absorption Measurements during a Sunspot Cycle," J. Atmosph. Terr. Phys., 5, 141-172, 1954.

Beynon, W. J. G. and Davies, K., "Simultaneous Ionospheric Absorption Measurements at Widely Separated Stations,'' J. Atmosph. Terr. Phys., 5, 273-289, 1954.

Bowhill, S. A., "The Ionosphere," Astronautics, 80-84, October, 1962.

Bowhill, S A. and Schmerling, E. R., "The Distribution of Electrons in the Ionosphere," Advances in Electronics and Electron Physics, 15, 265-324, 1961.

Bulman, G. R. P., "The Design of a New Apparatus for the Automatic Recording of High-Frequency Ionospheric Absorption; And a Study of the Effects of Focusing upon Absorption Measurements," The Pennsylvania State University, M.S.E.E. thesis, 1958.

Chapman, S., "The Absorption and Dissociative or Ionizing Effect of Monochromatic Radiation in an Atmosphere on a Rotating Earth," Proc. Phys, Soc., 43, 26-37, 1931.

Davies, K., "Ionospheric Radio Propagation," NBS Monograph 80, 1965.

Henry, G. W., to be published, 1965.

Jenkins, J. B. and Ratcliff, G., "The Investigation of Ionospheric Absorption by a New Automatic Method," Electronics Engineering, 25, 140-145, 1953.

Jordan, E. C., "Electromagnetic Waves and Radiating Systems," Prentice-Hall, Inc., Englewood-Cliffs, 1950.

Mitra, S. K., "The Upper Atmosphere," The Asiatic Society, Calcutta, 1952.

Piggott, W. R., Beynon, W. J. G., Brown, G. M. and Little, C. G., "The Measurement of Ionospheric Absorption," Annals of the IGY, 3, 175-226, 1957.

Piggott, W. R. and Brown, G. M. (editors), "Ionosphere," IQSY Instruction Manual No. 4, CIG-IQSY Committee, London, 1963.

Ratcliffe, J. A. (editor), "Physics of the Upper Atmosphere," Academic Press, New York, 1960.

Shapley, A. H. and Beynon, W. J. G., "Winter Anomaly in Ionospheric Absorption and Stratospheric Warmings," Nature, 206, 1242-1243, 1965.

Walston, J. A. and Miller, J. R. (editors), "Transistor Circuit Design," McGraw-Hill Book Co., Inc., New York, 1963.